symmetry

MDPI

Article

A New Asymmetric Modified Topp–Leone Distribution: Classical and Bayesian Estimations Under Progressive Type-II Censored Data with Applications

Mohammed Elgarhy [1,*], Najwan Alsadat [2], Amal S. Hassan [3,*], Christophe Chesneau [4] and Alaa H. Abdel-Hamid [1,*]

[1] Mathematics and Computer Science Department, Faculty of Science, Beni-Suef University, Beni-Suef 62521, Egypt
[2] Department of Quantitative Analysis, College of Business Administration, King Saud University, P.O. Box 71115, Riyadh 11587, Saudi Arabia; nalsadat@ksu.edu.sa
[3] Faculty of Graduate Studies for Statistical Research, Cairo University, 5 Dr. Ahmed Zewail Street, Giza 12613, Egypt
[4] Department of Mathematics, University de Caen Normandie, Campus II, Science 3, 14032 Caen, France; christophe.chesneau@unicaen.fr
* Correspondence: m_elgarhy85@sva.edu.eg (M.E.); amal52_soliman@cu.edu.eg (A.S.H.); hamid_alh@science.bsu.edu.eg (A.H.A.-H.)

Abstract: In this article, a new modified asymmetric Topp–Leone distribution is created and developed from a theoretical and inferential point of view. It has the feature of extending the remarkable flexibility of a special one-shape-parameter lifetime distribution, known as the inverse Topp–Leone distribution, to the bounded interval $[0,1]$. The probability density function of the proposed truncated distribution has the potential to be unimodal and right-skewed, with different levels of asymmetry. On the other hand, its hazard rate function can be increasingly shaped. Some important statistical properties are examined, including several different measures. In practice, the estimation of the model parameters under progressive type-II censoring is considered. To achieve this aim, the maximum likelihood, maximum product of spacings, and Bayesian approaches are used. The Markov chain Monte Carlo approach is employed to produce the Bayesian estimates under the squared error and linear exponential loss functions. Some simulation studies to evaluate these approaches are discussed. Two applications based on real-world datasets—one on the times of infection, and the second dataset is on trading economics credit rating—are considered. Thanks to its flexible asymmetric features, the new model is preferable to some known comparable models.

Keywords: maximum likelihood and Bayesian estimations; inverse Topp–Leone distribution; maximum product spacing estimation; Markov chain Monte Carlo; entropy and extropy; progressive type-II censoring

Citation: Elgarhy, M.; Alsadat, N.; Hassan, A.S.; Chesneau, C.; Abdel-Hamid, A.H. A New Asymmetric Modified Topp–Leone Distribution: Classical and Bayesian Estimations Under Progressive Type-II Censored Data with Applications. *Symmetry* **2023**, *15*, 1396. https://doi.org/10.3390/sym15071396

Academic Editors: Xinmin Li, Daojiang He and Weizhong Tian

Received: 15 June 2023
Revised: 30 June 2023
Accepted: 4 July 2023
Published: 10 July 2023

1. Introduction

The (probability) distributions with support $[0,1]$ play a crucial role in various fields. They allow us to model and analyze random events with limited outcomes, such as probabilities and proportions. They are vital in statistics, enabling us to estimate uncertainty and make informed decisions. Their significance extends to machine learning, where they aid in generating realistic data and estimating probabilities. Understanding and utilizing such distributions empowers us to grasp the inherent uncertainty of real-world phenomena accurately.

One of the most helpful existing distributions with support $[0,1]$ is the so-called Topp–Leone (TL) distribution with one shape parameter η, presented in [1]. The hazard rate function (HRF) of the TL distribution has great flexibility; it can be of bathtub shape or be of non-increasing shape, based on the values of the shape parameter η. For these reasons, it

is particularly successful for modelling lifetime data. Theoretically, its probability density function (PDF) is defined as

$$k(y;\eta) = 2\eta y^{\eta-1}(1-y)(2-y)^{\eta-1}, \quad 0 \le y \le 1, \eta > 0, \tag{1}$$

and $k(y;\eta) = 0$ for $y \notin [0,1]$, and the associated cumulative distribution function (CDF) is

$$K(y;\eta) = y^{\eta}(2-y)^{\eta}, \quad 0 \le y \le 1, \eta > 0, \tag{2}$$

and $K(y;\eta) = 0$ for $y < 0$ and $K(y;\eta) = 1$ for $y > 1$. The TL distribution and its extensions have received a lot of interest in the literature over the past few years. Among these extensions, there are the TL family of distributions introduced in [2–4], the transmuted TL-generated family proposed in [5], the Fréchet TL-generated family discussed in [6], the exponentiated generalized TL-generated family studied in [7], the new generalized TL-generated family explored in [8], the type-II TL-generated family discussed in [9], the new power TL-generated family proposed in [10], the power TL distribution proposed in [11], the odd log-logistic TL-generated family explored in [12] and the Burr III-TL-generated family discussed in [13].

Based on a random variable Y that follows the TL distribution, the authors of [14] employed the transformed random variable $Z = \frac{1}{Y} - 1$ and investigated its distributional and statistical properties. In particular, the distribution of Z, called the inverse TL (ITL) distribution, is defined by the following CDF and PDF, respectively:

$$G(z;\eta) = 1 - \left\{ \frac{(1+2z)^{\eta}}{(1+z)^{2\eta}} \right\}, \quad z \ge 0, \eta > 0, \tag{3}$$

and $G(z;\eta) = 0$ for $z < 0$, and

$$g(z;\eta) = 2\eta z(1+z)^{-2\eta-1}(1+2z)^{\eta-1}, \quad z \ge 0, \eta > 0, \tag{4}$$

where $g(z;\eta) = 0$ for $z < 0$. There are many advantages and reasons that motivate us to emphasize this distribution. We specify them as follows: (i) It is a very simple distribution with a closed form for its CDF; (ii) its PDF and HRF are unimodal and right-skewed; (iii) it has a closed form for the mode and quantiles, and these open the door for more statistical properties; (iv) since it has a single shape parameter, it is interesting for statisticians to use it in inference using different methods. In light these qualities, many authors considered Equations (3) and (4) to investigate new extensions of the ITL distribution, such as the new exponential ITL [15], new ITL [16] and truncated Cauchy power ITL [17] distributions.

On the other hand, by restricting the domain of any statistical distribution, a truncated distribution may be created. Therefore, when occurrences are limited to values above or below a specified threshold or within a particular range, truncated distributions are used. Ref. [18] discussed a truncated random variable Z on $[0,1]$ with the following PDF:

$$f(z) = \frac{g(z)}{G(1) - G(0)}, \quad z \in [0,1], \tag{5}$$

where $f(z) = 0$ for $z \notin [0,1]$, and $G(z)$ and $g(z)$ are the CDF and PDF on a distribution with support containing $[0,1]$. The associated CDF is obtained as

$$F(z) = \frac{G(z) - G(0)}{G(1) - G(0)}, \quad z \in [0,1], \tag{6}$$

where $F(z) = 1$ for $z > 1$ and $F(z) = 0$ for $z < 0$. Many statisticians have utilized Equations (5) and (6) to create new $[0,1]$ truncated distributions as well as new generating families of distributions. On this general topic, we may mention the truncated Fréchet-G family [19]. Furthermore, ref. [20] investigated the truncated inverted Kumaraswamy family.

Ref. [21] introduced the generalized truncated Fréchet-G family and [22] proposed a new truncated Muth-G family. This $[0, 1]$ truncated scheme, combined with the TIL distribution, will be at the heart of the article, as detailed more precisely after.

Furthermore, a clear statistical framework must be provided in order to motivate the statistical contributions of the present work. In the literature on life testing and reliability analysis, progressive type-II censoring (PCT-II) has recently received a lot of attention. The fundamental benefit of this censorship over conventional censoring type-II (CT-II) is that live units may be removed under it at intermediate stages, whereas under CT-II, live units may only be removed after the experiment is terminated. The process that follows can be used to obtain lifetime data under this scheme. Assume a sample of n distinct, identical units is placed through a life-test experiment. Assume further that unit lifetimes follow a common distribution with PDF $f(z;\theta)$ and CDF $F(z;\theta)$, where θ is a vector of unknown parameters. As the experiment progresses, test units will begin to fail. Let us assume that the first failure happens at a random time $Z_{(1)}$. Then, as a result of this censoring, at time $Z_{(1)}$, S_1 live units are eliminated from the experiment's remaining $n-1$ units. After the second failure, $Z_{(2)}$, units from the remaining $n-2-S_1$ are also randomly removed, and so on, with the experiment coming to an end when the r^{th} failure happens, all remaining $n-r-S_1-S_2-\ldots-S_{r-1}$ units are eliminated. Here, failure numbers r and censoring scheme $S=(S_1, S_2, \ldots, S_r)$ are predetermined and fixed. A useful description and good summary of progressive censoring (PC) can be found in [23–34]. It should be noted that, when $S_1 = S_2 = \ldots = S_{r-1} = 0$ and $S_r = n-r$, this censoring reduces to CT-II. Additionally, for $r = n$ and $S_i = 0$, $i = 1, 2, \ldots, n$, it reduces to a complete sample. Figure 1 represents this PC strategy.

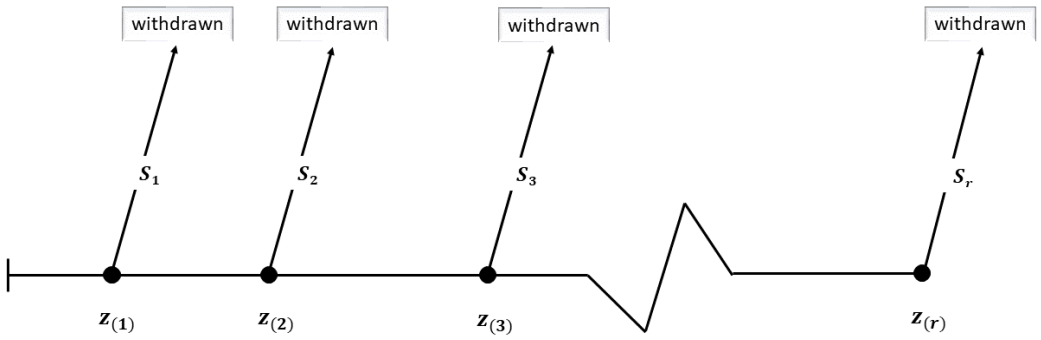

Figure 1. Presentation of the PCT-II scheme.

In light of the preceding paragraphs, we will focus our efforts in this article on a novel truncated distribution known as the truncated ITL (TITL) distribution. It is especially interesting for the following reasons: (i) It has a very simple PDF and CDF with only one shape parameter; (ii) its PDF can be unimodal, and right-skewed, reaching various levels of asymmetry; (iii) it has an increasing HRF; (iv) the corresponding mode and quantile have closed-form expressions; (v) some important statistical properties such as the mode, quantiles, median, Bowley's skewness, Moor's kurtosis, moments, incomplete moments, Lorenz and Bonferroni curves, and probability-weighted moments (PWMs) can be calculated; (vi) several different measures of uncertainty, such as the Rényi (RI) entropy, Tsallis (TS) entropy, Arimoto (AR) entropy, Havrda and Charvat (HC) entropy, Awad and Alawneh 1 (AA1) entropy, Awad and Alawneh 2 (AA2) entropy, Mathai–Haubold (MH) entropy, extropy, and residual extropy can be computed; (vii) different Bayesian and non-Bayesian estimation approaches under the PCT-II, such as the maximum likelihood (ML), maximum product of spacings (MPS), and Bayesian approach under the squared error (SE) loss function and linear exponential (LIN) loss function can be used efficiently to estimate the shape parameter of the TITL distribution; and (viii) on the practical side, we analyze two numerous datasets, showing that the TITL distribution can be a better alternative to strong competitors, such as the TL, power XLindley (PXL), inverse power Lindley (IPL),

Kumaraswamy (Kw), beta (B), truncated Weibull (TW), unit-Weibull (UW), exponentiated Kw (EKw), unit-Rayleigh (UR), Kavya–Manoharan Kw (KMKw) and transmuted Kw (TKw) distributions.

The rest of this article is organized as follows: Section 2 presents the construction of the TITL distribution. Several of its general properties are described in Section 3, with the help of graphics and numerical tables when appropriate. In Section 4, some measures of uncertainty are discussed. In Section 5, the classical methods of estimation, such as the ML and MPS methods, are examined under the PCT-II. In Section 6, the Bayesian estimation is proposed. Section 7 covers the simulation findings. Section 8 uses two real-world datasets to show the TITL distribution's applicability and flexibility. In addition, the conclusion is made at the end of the article in Section 9.

2. The New TITL Distribution

This section describes the main functions defining the TITL distribution. First, by employing Equations (3) and (4) into Equations (5) and (6), the associated PDF and CDF of the TITL distribution are given as

$$f(z;\eta) = \frac{2\eta}{A} z(1+z)^{-2\eta-1}(1+2z)^{\eta-1}, \quad z \in [0,1],\ \eta > 0, \tag{7}$$

where $A = 1-(0.75)^{\eta}$ and $f(z;\eta) = 0$ for $z \notin [0,1]$, and

$$F(z;\eta) = \frac{1}{A}\left[1 - \left\{\frac{(1+2z)^{\eta}}{(1+z)^{2\eta}}\right\}\right], \quad z \in [0,1],\ \eta > 0, \tag{8}$$

where $F(z;\eta) = 0$ for $z < 0$ and $F(z;\eta) = 1$ for $z > 1$, respectively. Another form of the PDF in Equation (7), which can make the calculation of the statistical and mathematical properties easy, can be written as follows:

$$f(z;\eta) = \frac{2\eta}{A} z(1+z)^{-\eta-2}\left(1+\frac{z}{1+z}\right)^{\eta-1}, \quad z \in [0,1],\ \eta > 0. \tag{9}$$

In power form, which is recommended for estimation purposes, we can write it as

$$f(z;\eta) = \frac{2\eta z}{A(1+2z)(1+z)}\left[\frac{1+2z}{(1+z)^2}\right]^{\eta}, \quad z \in [0,1],\ \eta > 0. \tag{10}$$

Furthermore, the survival function (SF), HRF, reversed HRF, and cumulative HRF are supplied by

$$S(z;\eta) = 1 - \frac{1}{A}\left[1 - \left\{\frac{(1+2z)^{\eta}}{(1+z)^{2\eta}}\right\}\right], \quad z \in [0,1],$$

where $S(z;\eta) = 1$ for $z < 0$,

$$h(z;\eta) = \frac{2\eta z(1+z)^{-2\eta-1}(1+2z)^{\eta-1}}{A - \left[1 - \left\{\frac{(1+2z)^{\eta}}{(1+z)^{2\eta}}\right\}\right]}, \quad z \in [0,1],$$

and $h(z;\eta) = 0$ for $z \notin [0,1]$,

$$\tau(z;\eta) = \frac{2\eta z(1+z)^{-2\eta-1}(1+2z)^{\eta-1}}{1 - \left\{\frac{(1+2z)^{\eta}}{(1+z)^{2\eta}}\right\}}, \quad z \in [0,1],$$

and $\tau(z;\eta) = 0$ for $z \notin [0,1]$, and

$$H(z;\eta) = -\log\left[1 - \frac{1}{A}\left[1 - \left\{\frac{(1+2z)^{\eta}}{(1+z)^{2\eta}}\right\}\right]\right], \quad z \in [0,1],$$

and $H(z;\eta) = 0$ for $z > 1$, respectively. The plots of the PDF and HRF are displayed in Figure 2. It can be noticed that the PDF can be uni-modal and right-skewed, with several degrees of asymmetry. In addition, the HRF can increase with "concave then convex" shapes. Figures 3 and 4 complete Figure 2; they show the 3D plots of the PDF and HRF with respect to z and η. We still observe that the PDF can be uni-modal and right-skewed, and that the HRF can be increasing in a smooth manner with respect to z and η.

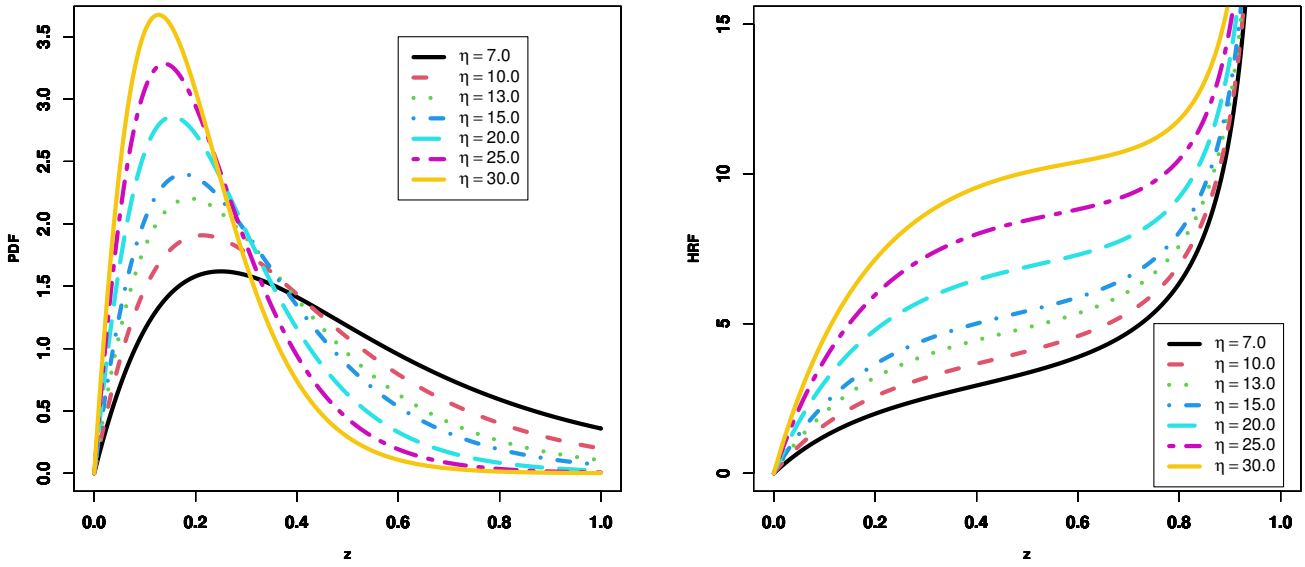

Figure 2. Plots of the PDF and HRF of the TITL distribution.

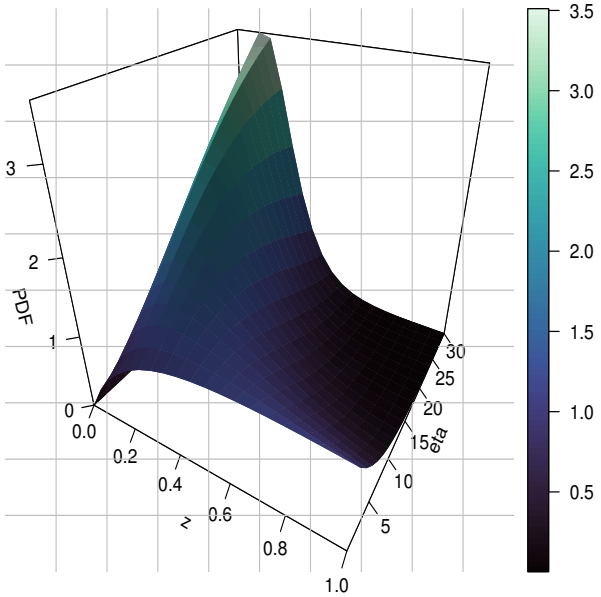

Figure 3. 3D plot of the PDF of the TITL distribution.

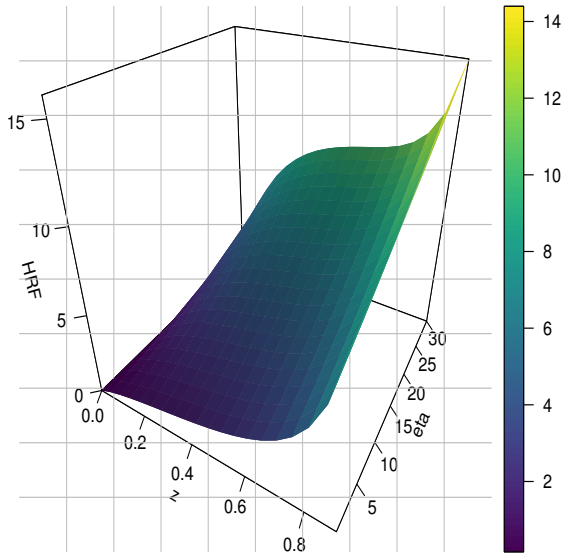

Figure 4. 3D Plot of the HRF of the TITL distribution.

3. General Statistical-Related Properties

In this section, we examine some general structural features of the TITL distribution.

3.1. Mode

A mode of the TITL distribution is a maximum point of the PDF in Equation (7). It can be identified by equating $\frac{d\log[f(z;\eta)]}{dz}$ with zero, as shown below:

$$\frac{d\log[f(z;\eta)]}{dz} = \frac{1}{z} - \frac{2\eta+1}{1+z} + \frac{2\eta-2}{1+2z} = 0. \tag{11}$$

After some simplifications, Equation (11) reduces to

$$2(\eta+1)z^2 - 1 = 0.$$

Then, the mode of the TITL distribution is unique, and it is simply given by

$$z_M = \frac{1}{\sqrt{2(1+\eta)}}. \tag{12}$$

Clearly, this result is an advantage of the TITL distribution. Indeed, the analytical expression of the mode facilitates the understanding and interpretation of the underlying distribution, enabling researchers and analysts to gain insights into the shape, symmetry, and potential clustering of the data. By identifying the mode, one can discern patterns, detect outliers, and make informed inferences about the data's characteristics, aiding in hypothesis testing and drawing meaningful conclusions.

3.2. Quantile Function

The quantile function is defined as $Q(u;\eta) = F^{-1}(u;\eta), u \in (0,1)$. It is naturally computed by inverting Equation (8) as

$$\frac{1}{A}\left[1 - \left\{\frac{(1+2Q(u;\eta))^{\eta}}{(1+Q(u;\eta))^{2\eta}}\right\}\right] = u.$$

After some algebraic simplifications, we arrive at

$$wQ(u;\eta)^2 + 2(w-1)Q(u;\eta) + w - 1 = 0,$$

where $w = (1-uA)^{\frac{1}{\eta}}$. By solving the above quadratic equation with respect to $Q(u;\eta)$ with the coefficients $a = w$, $b = 2(w-1)$ and $c = w - 1$, we obtain

$$Q(u;\eta) = \frac{1 - w + \sqrt{1-w}}{w}. \tag{13}$$

This simple expression is also an advantage of the TITL distribution. Indeed, having the analytical expression of the quantile function of a distribution provides precise and efficient calculation of specific percentiles, reducing computational complexity. Additionally, it allows for a deeper understanding of the distribution's behaviour and facilitates the analysis and interpretation of data. In particular, setting $u = 0.25$, 0.5, and 0.75 in Equation (13), we obtain the first (Q_1), second (median) (Q_2), and third (Q_3) quantiles. Moreover, based on the quantiles, Bowley's skewness (α_1) and Moor's kurtosis (α_2) are provided, respectively, by

$$\alpha_1 = \frac{Q(0.75;\eta) - 2Q(0.5;\eta) + Q(0.25;\eta)}{Q(0.75;\eta) - Q(0.25;\eta)},$$

and

$$\alpha_2 = \frac{Q(0.875;\eta) - Q(0.625;\eta) - Q(0.375;\eta) + Q(0.125;\eta)}{Q(0.75;\eta) - Q(0.25;\eta)}.$$

Some numerical values of the first, second (median), third quartiles, α_1 and α_2 are given in Table 1.

From Table 1, we can notice that when η increases, the values of Q_1, Q_2, and Q_3 decrease, but the values of α_1 and α_2 increase then decrease. Figures 5–7 show the 3D plots of Bowley's skewness, Moor's kurtosis and median. These figures support the numerical values in Table 1. We can notice that the median can be decreasing, but Bowley's skewness and Moor's kurtosis increase and then decrease.

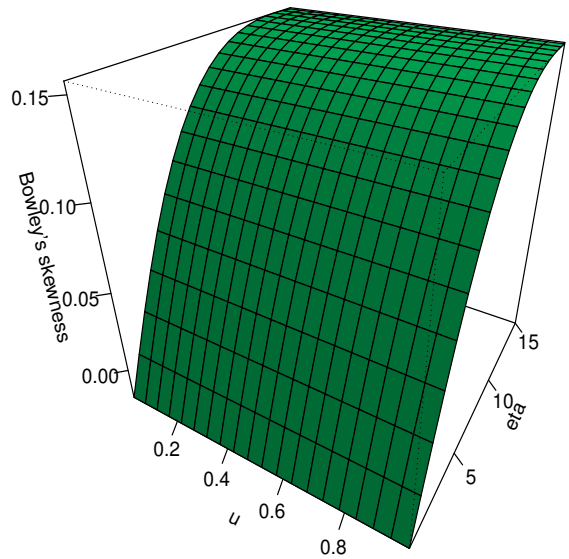

Figure 5. 3D Plot of Bowley's skewness for the TITL distribution.

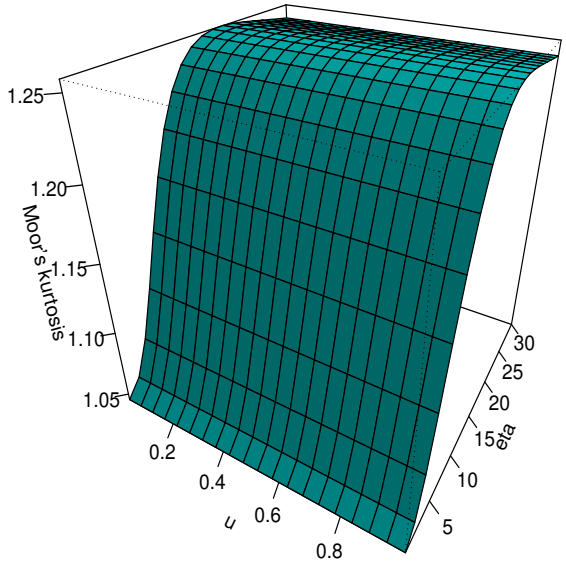

Figure 6. 3D Plot of Moor's kurtosis for the TITL distribution.

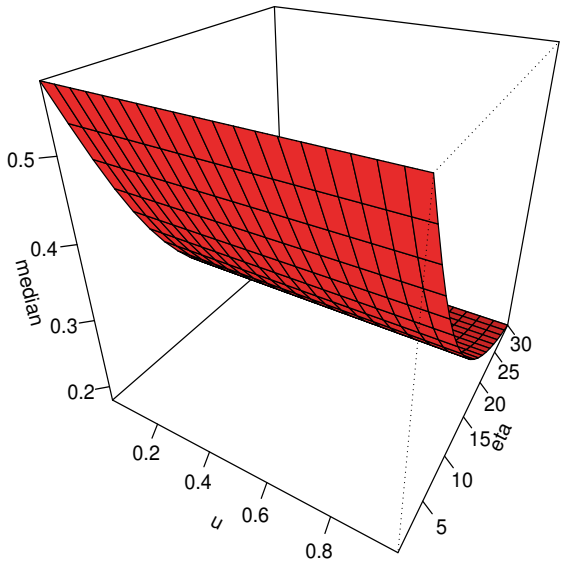

Figure 7. 3D Plot of the median for the TITL distribution.

Table 1. Numerical values of Q_1, Q_2, Q_3, α_1 and α_2 of the TITL distribution.

η	Q_1	Q_2	Q_3	α_1	α_2
2	0.311	0.517	0.738	0.036	1.06
5	0.256	0.434	0.653	0.103	1.117
7	0.227	0.387	0.595	0.13	1.162
10	0.195	0.331	0.516	0.151	1.215
13	0.171	0.289	0.45	0.156	1.244
15	0.158	0.267	0.415	0.155	1.253
20	0.135	0.226	0.348	0.149	1.256
25	0.12	0.198	0.302	0.142	1.252
27	0.115	0.189	0.288	0.14	1.25
30	0.108	0.178	0.27	0.136	1.248

3.3. Moments

Examining moments and moment measures of a distribution is crucial for understanding its properties and making informed decisions. They provide valuable insights into the central tendencies, spread, and shape of the data, aiding in statistical analysis and hypothesis testing. The rest of this section is devoted to these aspects.

Hereafter, we consider a random variable Z with the TITL distribution.

For any integer k, the k^{th} moment of Z is defined as

$$\mu'_k = E(Z^k) = \int_0^1 z^k f(z;\eta)dz = \frac{2\eta}{A}\int_0^1 z^{k+1}(1+z)^{-\eta-2}\left(1+\frac{z}{1+z}\right)^{\eta-1}dz. \tag{14}$$

For the integral in Equation (14), we have no a way to determine this integral in an algebraic manner. For this reason, we must investigate a manageable expansion of it.

To this end, let us recall the generalized binomial expansion. For any real non-integer $\zeta > 0$ and $|u| < 1$, we have

$$(1+u)^{\zeta} = \sum_{i=0}^{\infty}\binom{\zeta}{i}u^i. \tag{15}$$

We also have

$$(1+u)^{-\zeta} = \sum_{j=0}^{\infty}(-1)^j\binom{\zeta+j-1}{j}u^j. \tag{16}$$

By employing Equation (15) in the last term of Equation (14), we obtain

$$\mu'_k = \frac{2\eta}{A}\sum_{i=0}^{\infty}\binom{\eta-1}{i}\int_0^1 z^{k+i+1}(1+z)^{-\eta-i-2}dz. \tag{17}$$

On the other hand, by using Equation (16) in Equation (17), we obtain

$$\mu'_k = \sum_{i,j=0}^{\infty}\int_0^1 w_{i,j}z^{k+i+j+1}dz, \tag{18}$$

where $w_{i,j} = \frac{2\eta}{A}(-1)^j\binom{\eta+i+j+1}{j}\binom{\eta-1}{i}$.

Then the k^{th} moment of Z can be expanded as

$$\mu'_k = \sum_{i,j=0}^{\infty}\frac{w_{i,j}}{k+i+j+2}, \tag{19}$$

which is quite manageable from a computational viewpoint.

Furthermore, the k^{th} central moment (μ_k) of Z is given by

$$\mu_k = E[(Z-\mu'_1)^k] = \sum_{i=0}^{k}(-1)^i\binom{k}{i}(\mu'_1)^i\mu'_{k-i}.$$

Table 2 shows the numerical values of the first four moments μ'_1, μ'_2, μ'_3 and μ'_4, as well as the numerical values of the variance of Z (σ^2), coefficient of skewness of Z ($\gamma_1 = \frac{\mu_3}{\mu_2^{1.5}}$), coefficient of kurtosis of Z ($\gamma_2 = \frac{\mu_4}{\mu_2^2}$), coefficient of variation of Z ($CV = \frac{\sigma}{\mu'_1}$) and mode for the TITL distribution. From this table, as the values of η increase, the values of σ^2 and mode decrease, whereas γ_2 increases, but γ_1 and CV increase and then decrease. One can also observe that the TITL distribution is mainly right-skewed, leptokurtic (since $\gamma_2 > 3$), and platykurtic (since $\gamma_2 < 3$) .

Table 2. Results of some moments, γ_1, γ_2, CV and mode for the TITL distribution.

η	μ_1'	μ_2'	μ_3'	μ_4'	σ^2	γ_1	γ_2	CV	Mode
2	0.524	0.341	0.25	0.196	0.067	0.036	1.935	0.494	0.408
5	0.462	0.277	0.191	0.144	0.063	0.299	2.097	0.545	0.289
7	0.424	0.239	0.158	0.115	0.059	0.461	2.308	0.573	0.250
10	0.373	0.19	0.117	0.081	0.051	0.679	2.742	0.606	0.213
13	0.331	0.152	0.086	0.056	0.043	0.86	3.256	0.628	0.189
15	0.307	0.132	0.071	0.044	0.038	0.956	3.606	0.636	0.177
20	0.26	0.095	0.044	0.025	0.028	1.113	4.36	0.643	0.154
25	0.227	0.072	0.029	0.014	0.021	1.172	4.807	0.638	0.139
27	0.216	0.065	0.025	0.012	0.019	1.177	4.898	0.635	0.134
30	0.202	0.057	0.021	0.009	0.016	1.172	4.961	0.63	0.127

3.4. Incomplete Moments

The incomplete moments of a distribution hold valuable insights, capturing the dynamics beyond simple means and variances. They reveal the asymmetries and tails of the distribution, shedding light on extreme events and helping in risk assessment and decision making. Embracing these incomplete moments deepens our understanding of the underlying data, making them vital for robust statistical analysis.

For any integer k, the k^{th} lower incomplete moment of Z is computed from the following formula:

$$\Phi_k(t) = E(Z^k 1_{\{Z\leq t\}}) = \int_0^t z^k f(z;\eta)dz = \frac{2\eta}{A}\int_0^t z^{k+1}(1+z)^{-\eta-2}\left(1+\frac{z}{1+z}\right)^{\eta-1}dz, \;\; 0<t<1.$$

Thus, after algebraic developments similar to those employed for the k^{th} moment, the k^{th} lower incomplete moment of the TITL distribution is

$$\Phi_k(t) = \sum_{i,j=0}^{\infty} \frac{w_{i,j}t^{k+i+j+2}}{k+i+j+2}. \tag{20}$$

By applying $t \to \infty$, we obtain the k^{th} moment of Z.

Based on this, we can express the Lorenz (Ω_1) and Bonferroni (Ω_2) curves, which are essential in reliability, economics, medicine, demography, and insurance [35]. In the setting of the TITL distribution, they are computed as follows:

$$\Omega_1 = \frac{\Phi_1(t)}{E(Z)} = \frac{\sum\limits_{i,j=0}^{\infty} \frac{w_{i,j}t^{i+j+3}}{i+j+3}}{\sum\limits_{i,j=0}^{\infty} \frac{w_{i,j}}{i+j+3}},$$

and

$$\Omega_2 = \frac{\Omega_1}{F(t;\eta)} = \frac{\sum\limits_{i,j=0}^{\infty} \frac{w_{i,j}t^{i+j+3}}{i+j+3}}{\left(\sum\limits_{i,j=0}^{\infty} \frac{w_{i,j}}{i+j+3}\right)\left(\frac{1}{A}\left[1-\left\{\frac{(1+2t)^\eta}{(1+t)^{2\eta}}\right\}\right]\right)},$$

respectively.

3.5. Probability Weighted Moments

Probability-weighted moments (PWMs) play a crucial role in understanding the characteristics of a distribution. By incorporating both the probabilities and the values of a distribution, PWMs provide a comprehensive measure of the central tendency and dispersion, enabling more accurate analysis and decision making. Ref. [36] reported further

information on this subject. For any integers s and v, the $(s,v)^{th}$ PWM of Z is calculated as follows:

$$\tau_{s,v} = E[Z^s F(Z;\eta)^v] = \int_0^1 z^s F(z;\eta)^v f(z;\eta) dz. \tag{21}$$

As a direct calculation is not possible, we investigate a series expansion. Substituting Equations (8) and (9) into Equation (21), we obtain

$$\tau_{s,v} = \frac{2\eta}{A^{v+1}} \int_0^1 z^{s+1}(1+z)^{-\eta-2}\left(1+\frac{z}{1+z}\right)^{\eta-1}\left[1-\left\{\frac{(1+\frac{z}{1+z})^{\eta}}{(1+z)^{\eta}}\right\}\right]^v dz. \tag{22}$$

Since v is an integer, the standard binomial expansion gives

$$\left[1-\left\{\frac{(1+\frac{z}{1+z})^{\eta}}{(1+z)^{\eta}}\right\}\right]^v = \sum_{i=0}^{v}(-1)^i\binom{v}{i}\frac{(1+\frac{z}{1+z})^{\eta i}}{(1+z)^{\eta i}}. \tag{23}$$

By setting Equation (23) in Equation (22), we obtain

$$\tau_{s,v} = \frac{2\eta}{A^{v+1}} \sum_{i=0}^{v}(-1)^i\binom{v}{i} \int_0^1 z^{s+1}(1+z)^{-\eta(i+1)-1}\left(1+\frac{z}{1+z}\right)^{\eta(i+1)-1} dz. \tag{24}$$

By using the binomial expansion in Equation(15) in Equation (24), we obtain

$$\tau_{s,v} = \frac{2\eta}{A^{v+1}} \sum_{i=0}^{v}\sum_{j=0}^{\infty}(-1)^i\binom{v}{i}\binom{\eta(i+1)-1}{j} \int_0^1 z^{s+j+1}(1+z)^{-\eta(i+1)-j-1} dz.$$

By employing the binomial theory in Equation (16) in the above equation, we get

$$\tau_{s,v} = \sum_{i=0}^{v}\sum_{j,k=0}^{\infty} w_{i,j,k} \int_0^1 z^{s+j+k+1} dz,$$

where $w_{i,j,k} = \frac{2\eta}{A^{v+1}}(-1)^{i+k}\binom{v}{i}\binom{\eta(i+1)-1}{j}\binom{\eta(i+1)+j+k}{k}$.

Then the $(s,v)^{th}$ PWM of Z can be expanded as

$$\tau_{s,v} = \sum_{i=0}^{v}\sum_{j,k=0}^{\infty}\frac{w_{i,j,k}}{s+j+k+2}.$$

By taking $v=0$, we obtain the s^{th} moment of Z.

4. Measures of Uncertainty

The entropy of a distribution provides a measure of its unpredictability or information content. It is crucial in various fields such as information theory, statistical physics, and machine learning. A higher entropy implies greater uncertainty and diversity, fostering exploration, randomness, and robustness in systems. Different measures of entropy exist. Some of them are investigated below in the context of the TITL distribution.

4.1. Different Measures of Entropy

The RI entropy [37] of the TITL distribution is defined as follows:

$$R^{**}(\rho) = (1-\rho)^{-1}\log(\Delta), \tag{25}$$

where $\rho \neq 1, \rho > 0$ and $\Delta = \int_0^1 f(z;\eta)^\rho dz$. Furthermore, a direct calculation is not possible; therefore, we investigate a series expansion. The integral Δ is computed as follows:

$$\Delta = \left(\frac{2\eta}{A}\right)^\rho \int_0^1 z^\rho (1+z)^{-\rho(\eta+2)} \left(1+\frac{z}{1+z}\right)^{\rho(\eta-1)} dz.$$

By using binomial expansion in Equation (15) in the above equation, we obtain

$$\Delta = \left(\frac{2\eta}{A}\right)^\rho \sum_{i=0}^{\infty} \binom{\rho(\eta-1)}{i} \int_0^1 z^{\rho+i} (1+z)^{-\rho(\eta+2)-i} dz.$$

Furthermore, employing the binomial expansion in Equation (16), we get

$$\Delta = \sum_{i,j=0}^{\infty} \pi_{i,j} \int_0^1 z^{\rho+i+j} dz,$$

where $\pi_{i,j} = \left(\frac{2\eta}{A}\right)^\rho (-1)^j \binom{\rho(\eta-1)}{i} \binom{\rho(\eta+2)+i+j-1}{j}$. Then, we establish that

$$\Delta = \sum_{i,j=0}^{\infty} \frac{\pi_{i,j}}{\rho+i+j+1}. \tag{26}$$

By inserting Equation (26) into Equation (25), the RI entropy is

$$R^{**}(\rho) = (1-\rho)^{-1} \log\left[\sum_{i,j=0}^{\infty} \frac{\pi_{i,j}}{\rho+i+j+1}\right].$$

On the other hand, the next formula is utilized to calculate the TS entropy [38] of the TITL distribution:

$$T^{**}(\rho) = \frac{1}{\rho-1}(1-\Delta), \tag{27}$$

where $\rho \neq 1,\ \rho > 0$. By inserting Equation (26) into Equation (27), we obtain the TS entropy as follows:

$$T^{**}(\rho) = \frac{1}{\rho-1}\left[1 - \sum_{i,j=0}^{\infty} \frac{\pi_{i,j}}{\rho+i+j+1}\right].$$

The next formula, for $\rho \neq 1, \rho > 0$, is employed to compute the AR entropy [39] of the TITL distribution:

$$A^{**}(\rho) = \frac{\rho}{1-\rho}\left(\Delta^{\frac{1}{\rho}} - 1\right). \tag{28}$$

By employing Equation (26) in Equation (28), we obtain

$$A^{**}(\rho) = \frac{\rho}{1-\rho}\left[\left(\sum_{i,j=0}^{\infty} \frac{\pi_{i,j}}{\rho+i+j+1}\right)^{\frac{1}{\rho}} - 1\right].$$

For $\rho \neq 1, \rho > 0$, the HC entropy [40] of the TITL distribution is calculated as follows:

$$HC^{**}(\rho) = \frac{1}{2^{1-\rho}-1}\left(\Delta^{\frac{1}{\rho}} - 1\right). \tag{29}$$

Substituting Equation (26) into Equation (29), it is given by

$$HC^{**}(\rho) = \frac{1}{2^{1-\rho}-1}\left[\left(\sum_{i,j=0}^{\infty} \frac{\pi_{i,j}}{\rho+i+j+1}\right)^{\frac{1}{\rho}} - 1\right].$$

For $\rho \neq 1, \rho > 0$, the AA1 and AA2 entropies [41] of the TITL distribution are given, respectively, as

$$AA1^{**} = \frac{1}{\rho - 1} \log \left[\left[\sup_{0<z<1} f(z;\eta) \right]^{1-\rho} \Delta \right], \tag{30}$$

and

$$AA2^{**} = \frac{1}{2^{1-\rho} - 1} \left[\left\{ \left[\sup_{0<z<1} f(z;\eta) \right]^{1-\rho} \Delta \right\} - 1 \right], \tag{31}$$

where

$$\sup_{0<z<1} f(z;\eta) = f(z_M;\eta) = \frac{2\eta}{A} \left(\sqrt{2(1+\eta)} \right)^{\eta+1} \left(1 + \sqrt{2(1+\eta)} \right)^{-2\eta-1} \left(2 + \sqrt{2(1+\eta)} \right)^{\eta-1}.$$

By inserting Equation (26) in Equations (30) and (31), the AA1 and AA2 entropies are, respectively, given by

$$AA1^{**} = \frac{1}{\rho - 1} \log \left[f(z_M;\eta)^{1-\rho} \sum_{i,j=0}^{\infty} \frac{\pi_{i,j}}{\rho + i + j + 1} \right],$$

and

$$AA2^{**} = \frac{1}{2^{1-\rho} - 1} \left[\left\{ f(z_M;\eta)^{1-\rho} \sum_{i,j=0}^{\infty} \frac{\pi_{i,j}}{\rho + i + j + 1} \right\} - 1 \right].$$

For $\rho \neq 1, \rho < 2$, the MH entropy [42] of the TITL distribution is calculated as follows:

$$MH^{**}(\rho) = \frac{1}{\rho - 1} (\nabla - 1), \tag{32}$$

where

$$\nabla = \int_0^1 f(z;\eta)^{2-\rho} dz = \sum_{i,j=0}^{\infty} \frac{D_{i,j}}{3 - \rho + i + j}, \tag{33}$$

and $D_{i,j} = \left(\frac{2\eta}{A} \right)^{(2-\rho)} (-1)^j \binom{(2-\rho)(\eta-1)}{i} \binom{(2-\rho)(2\eta+1)+i+j-1}{j}$.

By inserting Equation (33) into Equation (32), it is given by

$$MH^{**}(\rho) = \frac{1}{\rho - 1} \left[\sum_{i,j=0}^{\infty} \frac{D_{i,j}}{3 - \rho + i + j} - 1 \right].$$

Table 3 displays some numerical measures of the introduced entropies. We conclude that:

- More variability is produced when the value of ρ increases, and for a fixed value of η, the values of R^{**}, HC^{**}, A^{**} and T^{**} decrease, resulting in more variability, whereas the values of $AA1^{**}$, $AA2^{**}$ and MH^{**} increase, resulting in more information.
- As the value of η increases and for a fixed value of ρ, the values of R^{**}, HC^{**}, A^{**}, T^{**} and MH^{**} decrease, resulting in more variability, but the values of $AA1^{**}$ decrease and then increase, while the values of $AA2^{**}$ increase and then decrease.

Table 3. Numerical values of entropy measures for the TITL distribution.

ρ	η	R^{**}	HC^{**}	A^{**}	T^{**}	$AA1^{**}$	$AA2^{**}$	MH^{**}
0.5	2	−0.026	−0.031	−0.025	−0.026	−0.177	0.223	−0.053
	5	−0.035	−0.042	−0.035	−0.035	−0.329	0.432	−0.088
	7	−0.055	−0.066	−0.054	−0.055	−0.426	0.573	−0.144
	10	−0.102	−0.120	−0.097	−0.100	−0.544	0.754	−0.261
	13	−0.163	−0.189	−0.150	−0.156	−0.627	0.888	−0.398
	15	−0.208	−0.239	−0.188	−0.198	−0.666	0.953	−0.493
	20	−0.329	−0.366	−0.280	−0.303	−0.722	1.049	−0.721
	25	−0.447	−0.484	−0.361	−0.401	−0.742	1.084	−0.925
	27	−0.492	−0.527	−0.389	−0.436	−0.744	1.089	−1.000
	30	−0.557	−0.587	−0.427	−0.486	−0.745	1.09	−1.104
0.8	2	−0.036	−0.048	−0.036	−0.036	−0.167	0.228	−0.046
	5	−0.052	−0.070	−0.052	−0.052	−0.312	0.433	−0.073
	7	−0.084	−0.112	−0.083	−0.083	−0.398	0.557	−0.118
	10	−0.153	−0.203	−0.150	−0.151	−0.493	0.697	−0.215
	13	−0.239	−0.313	−0.232	−0.233	−0.551	0.784	−0.328
	15	−0.300	−0.391	−0.289	−0.291	−0.574	0.819	−0.406
	20	−0.451	−0.580	−0.427	−0.431	−0.599	0.856	−0.592
	25	−0.589	−0.747	−0.547	−0.555	−0.600	0.858	−0.756
	27	−0.638	−0.806	−0.590	−0.599	−0.598	0.855	−0.814
	30	−0.708	−0.888	−0.649	−0.660	−0.594	0.848	−0.895
1.2	2	−0.046	−0.071	−0.046	−0.046	−0.156	0.238	−0.036
	5	−0.072	−0.113	−0.073	−0.073	−0.292	0.438	−0.052
	7	−0.117	−0.183	−0.118	−0.118	−0.365	0.543	−0.083
	10	−0.210	−0.331	−0.214	−0.215	−0.436	0.645	−0.151
	13	−0.317	−0.506	−0.326	−0.328	−0.472	0.696	−0.233
	15	−0.390	−0.627	−0.403	−0.406	−0.484	0.713	−0.291
	20	−0.560	−0.915	−0.587	−0.592	−0.490	0.722	−0.431
	25	−0.704	−1.167	−0.747	−0.756	−0.485	0.715	−0.555
	27	−0.754	−1.258	−0.804	−0.814	−0.482	0.711	−0.599
	30	−0.823	−1.383	−0.883	−0.895	−0.478	0.705	−0.660
1.5	2	−0.052	−0.090	−0.052	−0.053	−0.150	0.247	−0.026
	5	−0.086	−0.150	−0.087	−0.088	−0.278	0.444	−0.035
	7	−0.139	−0.246	−0.142	−0.144	−0.342	0.537	−0.055
	10	−0.246	−0.446	−0.256	−0.261	−0.400	0.619	−0.100
	13	−0.363	−0.680	−0.386	−0.398	−0.426	0.655	−0.156
	15	−0.441	−0.842	−0.475	−0.493	−0.433	0.665	−0.198
	20	−0.616	−1.231	−0.683	−0.721	−0.434	0.667	−0.303
	25	−0.760	−1.579	−0.865	−0.925	−0.429	0.659	−0.401
	27	−0.811	−1.706	−0.931	−1.000	−0.426	0.655	−0.436
	30	−0.879	−1.885	−1.022	−1.104	−0.422	0.650	−0.486

4.2. Measures of Extropy

Extropy is a brand-new uncertainty measurement recently established in [43] as the complement dual of entropy [44]. Using the total log scoring method, extropy may be utilized statistically to grade forecasting distributions. The extropy of the TITL distribution is defined as follows:

$$\xi = -\frac{1}{2}\int_0^1 f(z;\eta)^2 dz. \tag{34}$$

A series expansion is needed to have a computational aspect to this integral. By employing the PDF in Equation (9) in Equation (34) and after some simplifications, the extropy of the TITL distribution is given by

$$\xi = -\frac{1}{2}\left[\sum_{i,j=0}^{\infty} \frac{\nu_{i,j}}{i+j+3}\right],$$

where $\nu_{i,j} = \left(\frac{2\eta}{A}\right)^2 (-1)^j \binom{2(\eta-1)}{i} \binom{2\eta+i+j+3}{j}$.

The residual extropy was described in [45]. It is defined as

$$\xi_t = -\frac{1}{2S(t;\eta)^2} \int_t^1 f(z;\eta)^2 dz. \tag{35}$$

Using the PDF in Equation (9) in Equation (35), the residual extropy of the TITL distribution is given by

$$\xi_t = -\frac{1}{2S(t;\eta)^2} \left[\sum_{i,j=0}^{\infty} \frac{\nu_{i,j}(1-t^{i+j+3})}{i+j+3} \right].$$

Table 4 displays some numerical values of the proposed extropy measures. We conclude from Table 4 that:

- When the value of η increases, the values of the extropy and residual extropy decrease, providing more uncertainty.
- When the value of t increases and for a fixed value of η, the residual extropy decreases, leading to more variability.

Table 4. Numerical values of the extropy measures for the TITL distribution.

η	Extropy	Residual Extropy					
		$t = 0.1$	$t = 0.3$	$t = 0.5$	$t = 0.7$	$t = 0.8$	$t = 0.9$
2	−0.531	−0.564	−0.723	−1.010	−1.674	−2.505	−5.003
5	−0.556	−0.600	−0.778	−1.060	−1.707	−2.527	−5.014
7	−0.593	−0.648	−0.841	−1.115	−1.743	−2.552	−5.026
10	−0.671	−0.747	−0.970	−1.229	−1.817	−2.602	−5.051
13	−0.763	−0.866	−1.130	−1.374	−1.914	−2.668	−5.085
15	−0.827	−0.952	−1.249	−1.486	−1.991	−2.722	−5.112
20	−0.988	−1.176	−1.577	−1.808	−2.223	−2.884	−5.195
25	−1.142	−1.401	−1.928	−2.172	−2.504	−3.087	−5.301
27	−1.200	−1.491	−2.071	−2.325	−2.627	−3.178	−5.350
30	−1.284	−1.624	−2.287	−2.560	−2.823	−3.326	−5.429

5. Classical Estimation

The inferential aspect of the TITL distribution is explored in this section.

5.1. Maximum Likelihood Estimation

Assume that $z_{(1)} \leq z_{(2)} \leq \ldots \leq z_{(r)}$ represents a PCT-II sample of size r from a sample of size n with the TITL distribution, i.e., with the PDF in Equation (10), the CDF in Equation (8) and the censoring scheme $S_1, S_2, \ldots, S_r$. Then the likelihood function under the PCT-II sample is

$$\begin{aligned} L(\eta) &= c^{\circ} \prod_{i=1}^{r} f\left(z_{(i)};\eta\right) \left[1 - F\left(z_{(i)};\eta\right)\right]^{S_i} \\ &= c^{\circ} \prod_{i=1}^{r} \frac{2\eta z_{(i)}}{(1-(0.75)^{\eta})(1+2z_{(i)})(1+z_{(i)})} \left[\frac{1+2z_{(i)}}{(1+z_{(i)})^2}\right]^{\eta} \left[1 - \frac{1}{1-(0.75)^{\eta}} \left[1 - \left(\frac{1+2z_{(i)}}{(1+z_{(i)})^2}\right)^{\eta}\right]\right]^{S_i}, \end{aligned} \tag{36}$$

where $c^{\circ} = n(n-S_1-1)(n-S_1-S_2-2)\ldots n-r+1-\sum_{i=1}^{r-1} S_i$. As a result, the constant is the number of different ways in which the r PCT-II order statistics might arise if the

observed failure times are $z_{(1)}, z_{(2)}, \ldots, z_{(r)}$. The log-likelihood function of Equation (36) is given by

$$\begin{aligned}\mathscr{L} = \log L(\eta) &= r\log 2c^{\circ} + r\log\eta - r\log(A) + \sum_{i=1}^{r}\log[C_i] \\ &+\eta\sum_{i=1}^{r}\log(B_i) + \sum_{i=1}^{r} S_i \log\Big[\Big[1 - A^{-1}\big[1-(B_i)^{\eta}\big]\Big]\Big],\end{aligned} \tag{37}$$

where $A = 1-(0.75)^{\eta}$, $B_i = \frac{1+2z_{(i)}}{(1+z_{(i)})^2}$ and $C_i = \frac{z_{(i)}}{(1+2z_{(i)})(1+z_{(i)})}$. Here, we present the ML estimate (MLE) of η denoted as $\hat{\eta}$, reporting that it is defined by maximizing the log-likelihood function. A derivative is just a technique to obtain it, not essential to the method. From Equation (37), we derive the first partial derivative for $\mathscr{L}$ with respect to η as

$$\frac{d\mathscr{L}}{d\eta} = \frac{r}{\eta} - \frac{rE}{A} + \sum_{i=1}^{r}\log(B_i) + \sum_{i=1}^{r}\frac{S_i D_i}{F_i} + \sum_{i=1}^{r}\frac{S_i G_i}{F_i}, \tag{38}$$

where $E = \frac{dA}{d\eta} = -(0.75)^{\eta}\log(0.75)$, $D_i = A^{-1}E\big[1-(B_i)^{\eta}\big]$, $F_i = A + (B_i)^{\eta} - 1$, and $G_i = (B_i)^{\eta}\log(B_i)$. Solving non-linear Equation (38) after setting it to zero, the MLE of η can be found using the Newton–Raphson iteration technique.

The theoretical findings presented above can be further specialized in one situation. First, the MLE $\hat{\eta}$ is yielded when $S_1 = S_2 = \ldots = S_{r-1} = 0$ and $S_r = n - r$ via CT-II samples. Second, we obtain the recommended MLE of η for $S_1 = S_2 = \ldots = S_r = 0$ via complete samples.

Now, the asymptotic variance–covariance matrix (V-CM) of $\hat{\eta}$ can be obtained by inverting the observed information matrix with the elements that are negative of the expected values of the second-order derivatives of logarithms of the likelihood function taken at the considered random sample. Thus, it is defined by

$$I(\eta) = \Big[-\mathrm{E}\big(\tfrac{d^2\mathscr{L}}{d\eta^2}\big)\Big],$$

where considering the observations instead of the random variable versions, we have

$$\frac{d^2\mathscr{L}}{d\eta^2} = -\frac{r}{\eta^2} - \frac{r\big(JA - E^2\big)}{A^2} + \sum_{i=1}^{r}\frac{S_i(H_iF_i - D_iK_i)}{{F_i}^2} + \sum_{i=1}^{r}\frac{S_i(M_iF_i - G_iK_i)}{{F_i}^2},$$

and $J = \frac{dE}{d\eta} = E\log(0.75)$, $H_i = \frac{dD_i}{d\eta} = -A^{-1}E^2D_i + \frac{JD_i}{E} - A^{-1}EG_i$, $K_i = \frac{dF_i}{d\eta} = E + G_i$, and $M_i = \frac{dG_i}{d\eta} = G_i\log(B_i)$.

Ref. [46] concluded that the approximation V-CM might be constructed by substituting anticipated values for their MLEs. The estimated sample information matrix is now generated as

$$I(\hat{\eta}) = -\Big[\tfrac{d^2\mathscr{L}}{d\eta^2}\Big], \tag{39}$$

and hence the approximation of V-CM of $\hat{\eta}$ is

$$\big[\sigma_{11}\big] = -\Big[\tfrac{d^2\mathscr{L}}{d\eta^2}\Big]^{-1}_{\eta=\hat{\eta}}. \tag{40}$$

Based on the subjacent distribution of the MLE of η, the confidence interval (CI) for η is computed. It is established from the empirical distribution of the MLE of η that $(\hat{\eta}) - (\eta) \rightarrow N\big(0, I^{-1}(\hat{\eta})\big)$, where $N(\cdot)$ is the normal distribution and $I(\cdot)$ is the Fisher information matrix (FIM) which is defined in Equation (39).

Considering specific regularity constraints, the two-sided $100(1-\gamma)\%, 0 < \gamma < 1$, asymptotic CI (Asy-CI) for η can be obtained as $\hat{\eta} \pm Z_{\frac{\gamma}{2}}\sqrt{\sigma_{11}}$, where σ_{11} is the asymptotic variance of the MLE of η, and $Z_{\frac{\gamma}{2}}$ is the upper $\frac{\gamma}{2}^{th}$ percentile of the standard normal distribution.

5.2. Maximum Product of Spacings Estimation

The MPS approach was established by Cheng and Amin [47]. It is crucial in statistical analysis for its ability to estimate the distribution parameters with high accuracy. By maximizing the product of the ordered spacings between data points, it provides robust estimates. In addition, the MPS estimate (MPSE) preserves most of the attributes of the MLE, including the invariance property (see [48,49]). Based on a PCT-II sample, according to [50], the MPS function may be expressed as follows:

$$M(\eta) = \prod_{i=1}^{r+1} \left[F\left(z_{(i)}, \eta\right) - F\left(z_{(i-1)}, \eta\right) \right] \prod_{i=1}^{r} \left[1 - F\left(z_{(i)}, \eta\right) \right]^{S_i}. \tag{41}$$

It may be calculated using Equations (8) and (41) as follows:

$$M(\eta) = A^{-r-1} \prod_{i=1}^{r+1} \left[(B_{i-1})^{\eta} - (B_i)^{\eta} \right] \prod_{i=1}^{r} \left[1 - A^{-1} \left[1 - (B_i)^{\eta} \right] \right]^{S_i}. \tag{42}$$

The natural logarithm of Equation (42), represented by $\log M(\eta)$, has the following form:

$$\log M(\eta) = -(r+1)\log(A) + \sum_{i=1}^{r+1} \log \left[(B_{i-1})^{\eta} - (B_i)^{\eta} \right] + \sum_{i=1}^{r} S_i \log \left[1 - A^{-1} \left[1 - (B_i)^{\eta} \right] \right]. \tag{43}$$

The MPSE maximizes the MPS function, and it can be obtained by differentiating Equation (43) with respect to η. The MPSE of η, denoted by $\tilde{\eta}$, is derived by concurrently solving the following equation:

$$\frac{d[\log M(\eta)]}{d\eta} = -\frac{-(r+1)E}{A} + \frac{G_{i-1} - G_i}{(B_{i-1})^{\eta} - (B_i)^{\eta}} + \sum_{i=1}^{r} \frac{S_i D_i}{F_i} + \sum_{i=1}^{r} \frac{S_i G_i}{F_i} = 0,$$

where $B_{i-1} = \frac{1+2z_{(i-1)}}{(1+z_{(i-1)})^2}$ and $G_{i-1} = (B_{i-1})^{\eta} \log(B_{i-1})$.

The MPSE $\tilde{\eta}$ may be obtained using the Newton–Raphson iteration approach.

6. Bayesian Estimation

In Bayesian inference, it is supposed that the unknown parameters are random variables with a joint prior density function. The prior density function may be calculated using previous information and experience. When no prior information is available, non-informative priors can be used for Bayesian inference. Here, we suppose that η is a gamma random variable having a prior density as follows:

$$\pi(\eta) = \eta^{a_1 - 1} e^{-b_1 \eta}, \quad \eta > 0. \tag{44}$$

In this formula, the hyperparameters a_1 and b_1 are employed to reflect previous knowledge of the unknown parameter.

The informative prior is used to elicit the hyperparameters. The above informative priors will indeed be deduced from the MLE for η by equating the mean and variance of $\hat{\eta}^j$ with both the mean and variance of the regarded gamma priors, where $j = 1, 2, \ldots, d$ and d is the number of available observations from the TITL distribution. Thus, according to [51], equating the mean and variance of $\hat{\eta}^j$ with the mean and variance of the gamma priors, we acquire

$$\frac{1}{d} \sum_{j=1}^{d} \hat{\eta}^j = \frac{a_1}{b_1} \qquad \text{and} \qquad \frac{1}{d-1} \sum_{j=1}^{d} \left(\hat{\eta}^j - \frac{1}{d} \sum_{j=1}^{d} \hat{\eta}^j \right)^2 = \frac{a_1}{b_1^2}.$$

After solving the above equations, the derived hyperparameters are

$$a_1 = \frac{\left(\frac{1}{d}\sum_{j=1}^{d}\hat{\eta}^j\right)^2}{\frac{1}{d-1}\sum_{j=1}^{d}\left(\hat{\eta}^j - \frac{1}{d}\sum_{j=1}^{d}\hat{\eta}^j\right)^2} \quad \text{and} \quad b_1 = \frac{\frac{1}{d}\sum_{j=1}^{d}\hat{\eta}^j}{\frac{1}{d-1}\sum_{j=1}^{d}\left(\hat{\eta}^j - \frac{1}{d}\sum_{j=1}^{d}\hat{\eta}^j\right)^2}.$$

In the case of non-informative priors (Non-IP), the Bayesian estimate (BE) is achieved by determining the hyperparameters $a_1 = b_1 = 0$ and using the same Markov chain Monte Carlo (MCMC) technique.

The following formula may be used to generate the posterior distribution of η:

$$\pi^*(\eta \mid \underline{z}) = \frac{\pi(\eta)\, L(\eta)}{\int_0^\infty \pi(\eta)\, L(\eta)\, d\eta}, \tag{45}$$

where $\underline{z} = (z_1, \ldots, z_n)$. The SE loss function is taken into account as a symmetrical loss function that indicates an equal loss due to overestimation and underestimation. The posterior distribution is obtained by

$$\begin{aligned}\pi^*(\eta \mid \underline{z}) \propto 2^r \eta^{r+a_1-1} e^{-b_1\eta} \prod_{i=1}^{r} \frac{z_{(i)}}{(1-(0.75)^\eta)(1+2z_{(i)})(1+z_{(i)})} \left[\frac{1+2z_{(i)}}{(1+z_{(i)})^2}\right]^\eta \\ \times \left[1 - \frac{1}{1-(0.75)^\eta}\left[1 - \left(\frac{1+2z_{(i)}}{(1+z_{(i)})^2}\right)^\eta\right]\right]^{S_i}.\end{aligned} \tag{46}$$

Based on the SE loss function, the BE of η, say $\hat{\eta}_{SE}$, is as follows:

$$\hat{\eta}_{SE} = E[\eta \mid \underline{z}] = \left[\int_0^\infty \eta \pi^*(\eta \mid \underline{z}) d\eta\right]. \tag{47}$$

Based on the LIN loss function, the BE of η, say $\hat{\eta}_{LIN}$, is as follows:

$$\hat{\eta}_{LIN} = -\frac{1}{\tau}\log E\left[e^{-\tau\eta} \mid \underline{z}\right] = -\frac{1}{\tau}\log\left[\int_0^\infty e^{-\tau\eta}\pi^*(\eta \mid \underline{z}) d\eta\right]. \tag{48}$$

Nevertheless, because the posterior in Equation (46) is not in a standard form, Gibbs sampling is not a viable alternative. As a result, for the MCMC approach to be implemented, Metropolis–Hastings (M-H) sampling is necessary. The M-H algorithm stages are expressed as follows:

1. Start with initial values $\eta^{(0)} = \hat{\hat{\eta}}_{ML}$.
2. Let $j = 1$.
3. Use the M-H algorithm to generate $\eta^{(j)}$ from $\pi^*\left(\eta^{(j-1)} \mid \underline{z}\right)$ with the normal distributions $N\left(\eta^{(j-1)}, S_\eta\right)$.
4. Generate a required η^* from $N\left(\eta^{(j-1)}, S_\eta\right)$. The choices of S_η are thought to be the asymptotic V-CM, say $I^{-1}\left(\hat{\eta}_{ML}\right)$, where $I(.)$ is the FIM.
   (i) Find the acceptance probabilities
   $$\Omega_\eta = \min\left[1, \frac{\pi^*(\eta^* \mid \underline{z})}{\pi^*\left(\eta^{(j-1)} \mid \underline{z}\right)}\right].$$
   (ii) From the uniform $[0, 1]$ distribution, generate the value u_1.
   (iii) If $u_1 < \Omega_\eta$, accept the proposal and set $\eta^{(j)} = \eta^*$; otherwise set $\eta^{(j)} = \eta^{(j-1)}$.
5. Set $j = j + 1$.
6. Repeat steps (3)–(5) N times, and obtain $\eta^{(i)}$, $i = 1, 2, \ldots N$.

7. To compute the credible CI (C-CI) of $\eta^{(i)}$ as $\eta^{(1)} < \eta^{(2)} \ldots < \eta^{(N)}$, then the $100(1-\gamma)\%$ C-CI of η is $\left(\eta_{(N\,\gamma/2)}, \eta_{(N\,(1-\gamma/2))}\right)$.

To assure convergence and remove the bias of initial value choice, the first M simulated variations are deleted. The chosen samples are then $\eta^{(i)}$, $j = M+1, \ldots N$, for sufficiently large N. The approximate BE of η depending on the SE loss function is supplied by

$$\hat{\eta} = \frac{1}{N-M} \sum_{j=M+1}^{N} \eta^{(j)}. \tag{49}$$

7. Numerical Outcomes

Here, Monte Carlo simulations utilizing PCT-II samples are presented to contrast the efficiency of the MLEs and MPSEs in non-BE on the one hand and the efficiency of the BEs employing MCMC under the SE and LIN loss functions at $\tau = 0.5$ and $\tau = -0.5$ on the other. The simulation results are examined and produced in terms of the average (Avg) estimates, root-mean-squared error (RMSE), relative bias (RB), the average length (AL) under Asy-CI/C-CI, and coverage probabilities (CPs). We obtain the MLEs, MPSEs and the BEs under the SE and LIN loss functions and choose four schemes, namely Scheme 1 (Sch.1), Scheme 2 (Sch.2), Scheme 3 (Sch.3), and Scheme 4 (Sch.4) from PCT-II samples with numerous values of (n, r)= (100, 50), (100, 70), (200, 100) and (200, 140) for η =1.5 and 3.0. The estimates are derived by taking into account the four censoring schemes listed below.

1. Sch.1: $S_1 = n - r$ and $S_2 = \ldots = S_r = 0$.
2. Sch.2: $S_1 = \frac{n-r}{2}$, $S_2 = \ldots = S_{r-1} = 0$ and $S_r = \frac{n-r}{2}$.
3. Sch.3: $S_1 = \ldots = S_{\frac{r}{2}-1} = 0$, $S_{\frac{r}{2}} = \frac{n-r}{2}$, $S_{\frac{r}{2}+1} = \frac{n-r}{2}$ and $S_{\frac{r}{2}+2} = \ldots = S_r = 0$, where r is an even number.
4. Sch.4: $S_1 = \ldots = S_{r-1} = 0$ and $S_r = n - r$.

We generate 10,000 MCMC samples with a burn-in duration of 2000 to acquire the BEs using the SE loss function. The procedure is repeated 1000 times. For computations, we utilized *R*, a statistical programming language. From Tables 5–8, it is observed that:

(a) For the non-BE

1. The RMSE and AL decrease when r increases for the ML and MPS approaches.
2. In almost all situations, using the MPS, the RMSE of $\tilde{\eta}$ is smaller than the MSE of $\hat{\hat{\eta}}$ using ML.
3. In almost all situations, using the ML, the RB of $\hat{\hat{\eta}}$ is smaller than the RB of $\tilde{\eta}$ using MPS.
4. In most situations, using the ML, Sch.4 gives the lowest value of the MSE for $\hat{\hat{\eta}}$.
5. In most situations, using the ML, Sch.3 gives the lowest value of the RB for $\hat{\hat{\eta}}$.
6. In most situations, using the MPS, Sch.4 gives the smallest values of the RMSE and RB for $\tilde{\eta}$.
7. The CP is greater than or equal 91.30% at $\gamma = 0.05$.
8. In almost all situations, using the ML, Sch.4 gives the smallest AL for η.
9. In almost all situations, using the MPS, Sch.4 gives the smallest AL for η.

(b) For the BE

1. The RMSE decreases when r increases for the MCMC method using the SE and LIN loss functions.
2. The AL decreases when r increases for the MCMC method using the SE and LIN loss functions.
3. In almost all situations, the RMSE and RB of $\hat{\eta}$ using the IP is less than the RMSE of $\hat{\eta}$ using the non-IP under the MCMC method using the SE and LIN loss functions.
4. The RMSE of $\hat{\eta}_{LIN}$ at $\tau = 0.5$ is less than the RMSE of $\hat{\eta}_{LIN}$ at $\tau = -0.5$ in most of situations for the IP and non-IP.

5. The RB of $\hat{\eta}_{LIN}$ at $\tau = -0.5$ is less than the RB of $\hat{\eta}_{SE}$, and $\hat{\eta}_{LIN}$ at $\tau = 0.5$, in almost all situations, for the non-IP.
6. In almost all situations, the RB of $\hat{\eta}_{SE}$ is less than the RB of $\hat{\eta}_{LIN}$ at $\tau = 0.5$ and $\tau = -0.5$ for the IP.
7. In almost all situations, using the MCMC under the non-IP, Sch.4 gives the smallest values of the RMSE for $\hat{\eta}$.
8. In almost all situations, using the MCMC under the non-IP, Sch.2 gives the smallest values of the RB for $\hat{\eta}$.
9. In the majority of situations, the RB of $\hat{\eta}_{LIN}$ at $\tau = 0.5$ is less than the RMSE of $\hat{\eta}_{SE}$ and $\hat{\eta}_{LIN}$ at $\tau = -0.5$ for the IP and non-IP.
10. In almost all situations, using the MCMC under the IP, Sch.4 gives the smallest values of the RMSEs for $\hat{\eta}$.
11. In almost all situations, using the MCMC under the IP, Sch.3 gives the smallest values of the RB for $\hat{\eta}$.
12. The CP is more than or equal 95.0% at $\gamma = 0.05$.
13. In almost all situations, using the MCMC under the non-IP, Sch.2 gives the lowest AL for η.
14. In almost all situations, using the MCMC under the IP, Sch.4 gives the lowest AL for η.
15. In almost all situations, using the MCMC, the AL under the IP is less than the AL under the non-IP for η.
16. In almost all situations, using the MCMC, the RMSE under the IP is less than the RMSE using the ML and MPS.
17. In almost all situations, using the MCMC, the RB under the IP is less than the RB using the ML and MPS.
18. In almost all situations, using the MCMC, the AL under the IP is less than the AL under the ML and MPS for η.

Table 5. Point estimation at $\eta = 1.5$.

(n, r)	Sch.	Measures	Non-Bayesian		Bayesian					
					Non-IP			IP		
			ML	MPS	SE	LIN		SE	LIN	
						$\tau = 0.5$	$\tau = -0.5$		$\tau = 0.5$	$\tau = -0.5$
$(100, 50)$	Sch.1	Avg	1.7694	1.8546	1.1726	1.0625	1.2905	1.6736	1.6148	1.8143
		RMSE	1.6327	1.6299	1.7446	1.6739	1.8287	1.3017	1.2445	1.3564
		RB	0.1796	0.2364	0.2183	0.2900	0.1400	0.1157	0.0800	0.2100
	Sch.2	Avg	1.6812	1.6661	0.9769	0.8560	1.1097	1.5611	1.4730	1.6610
		RMSE	1.2507	1.1929	1.4258	1.3867	1.4812	0.9954	0.9397	1.0680
		RB	0.1208	0.1107	0.3487	0.4300	0.2600	0.0407	0.0200	0.1100
	Sch.3	Avg	1.7016	1.8839	1.0272	0.9106	1.1593	1.6430	1.5266	1.7421
		RMSE	1.4085	1.3915	1.5492	1.5102	1.6084	1.1102	1.0653	1.1701
		RB	0.1344	0.2559	0.3152	0.3900	0.2300	0.0953	0.0200	0.1600
	Sch.4	Avg	1.6995	1.7175	1.0276	0.9111	1.1610	1.4931	1.4370	1.6328
		RMSE	1.2424	1.1621	1.4444	1.4211	1.4853	1.0441	1.0001	1.0809
		RB	0.1330	0.1450	0.3149	0.3900	0.2300	0.0046	0.0400	0.0900

Table 5. *Cont.*

(n, r)	Sch.	Measures	Non-Bayesian		Bayesian					
					Non-IP			IP		
			ML	MPS	SE	LIN		SE	LIN	
						$\tau = 0.5$	$\tau = -0.5$		$\tau = 0.5$	$\tau = -0.5$
(100, 70)	Sch.1	Avg	1.5696	1.6641	0.9890	0.8983	1.0885	1.5629	1.4895	1.6885
		RMSE	1.3337	1.2882	1.5135	1.4817	1.5554	1.0253	0.9627	1.0877
		RB	0.0464	0.1094	0.3407	0.4000	0.2700	0.0419	0.0100	0.1300
	Sch.2	Avg	1.6398	1.7147	1.0468	0.9462	1.1554	1.6197	1.5064	1.7123
		RMSE	1.1640	1.1310	1.3791	1.3523	1.4140	1.0063	0.9712	1.0716
		RB	0.0932	0.1431	0.3021	0.3700	0.2300	0.0798	0.0000	0.1400
	Sch.3	Avg	1.5682	1.6259	0.9768	0.8728	1.0902	1.5582	1.5166	1.6445
		RMSE	1.2199	1.2100	1.3919	1.3636	1.4350	1.0381	0.9891	1.0736
		RB	0.0455	0.0839	0.3488	0.4200	0.2700	0.0388	0.0100	0.1000
	Sch.4	Avg	1.5909	1.6244	1.0180	0.9260	1.1191	1.5809	1.5248	1.7182
		RMSE	1.2355	1.1635	1.4526	1.4209	1.4955	0.9692	0.9179	0.9983
		RB	0.0606	0.0829	0.3213	0.3800	0.2500	0.0540	0.0200	0.1500
(200, 100)	Sch.1	Avg	1.5914	1.6617	1.0325	0.9343	1.1392	1.4841	1.4393	1.6312
		RMSE	1.1465	1.0981	1.3969	1.3737	1.4320	0.9343	0.8840	0.9596
		RB	0.0610	0.1078	0.3116	0.3800	0.2400	0.0106	0.0400	0.0900
	Sch.2	Avg	1.6240	1.6316	1.0430	0.9455	1.1482	1.6870	1.6031	1.7511
		RMSE	1.0374	0.9869	1.2554	1.2428	1.2776	0.9575	0.9037	1.0206
		RB	0.0827	0.0878	0.3046	0.3700	0.2300	0.1247	0.0700	0.1700
	Sch.3	Avg	1.4956	1.6016	0.9448	0.8546	1.0418	1.4674	1.3837	1.5495
		RMSE	1.0593	0.9811	1.2496	1.2410	1.2673	0.8229	0.8043	0.8590
		RB	0.0030	0.0677	0.3701	0.4300	0.3100	0.0217	0.0800	0.0300
	Sch.4	Avg	1.5119	1.5242	0.9381	0.8393	1.0469	1.4186	1.3454	1.4571
		RMSE	0.9886	0.9308	1.2163	1.2159	1.2264	0.8380	0.8210	0.8848
		RB	0.0079	0.0161	0.3746	0.4400	0.3000	0.0543	0.1000	0.0300
(200, 140)	Sch.1	Avg	1.5384	1.6169	0.8937	0.8034	0.9924	1.4882	1.3955	1.5833
		RMSE	1.0634	0.9900	1.2371	1.2285	1.2574	0.8772	0.8564	0.9154
		RB	0.0256	0.0780	0.4042	0.4600	0.3400	0.0079	0.0700	0.0600
	Sch.2	Avg	1.5997	1.6211	0.9914	0.8996	1.0920	1.4423	1.3615	1.5286
		RMSE	0.9215	0.9025	1.1910	1.1917	1.1980	0.8258	0.8060	0.8574
		RB	0.0665	0.0807	0.3391	0.4000	0.2700	0.0385	0.0900	0.0200
	Sch.3	Avg	1.5219	1.5614	0.8847	0.7977	0.9802	1.4203	1.3354	1.4787
		RMSE	0.9114	0.8739	1.1818	1.1836	1.1906	0.7534	0.7431	0.7858
		RB	0.0146	0.0409	0.4102	0.4700	0.3500	0.0531	0.1100	0.0100
	Sch.4	Avg	1.4641	1.4990	0.8610	0.7822	0.9460	1.4294	1.3860	1.4859
		RMSE	0.9213	0.8396	1.1646	1.1714	1.1643	0.7557	0.7247	0.7723
		RB	0.0239	0.0007	0.4260	0.4800	0.3700	0.0471	0.0800	0.0100

Table 6. Point estimation at $\eta = 3.0$.

(n, r)	Sch.	Measures	Non-Bayesian		Bayesian					
					Non-IP			IP		
			ML	MPS	SE	LIN		SE	LIN	
						$\tau = 0.5$	$\tau = -0.5$		$\tau = 0.5$	$\tau = -0.5$
$(100, 50)$	Sch.1	Avg	3.1857	3.3117	2.5174	2.3583	2.6805	3.0145	2.8488	3.1843
		RMSE	1.6952	1.7022	2.2439	2.2420	2.2573	1.1379	1.1050	1.2020
		RB	0.0619	0.1039	0.1609	0.2100	0.1100	0.0048	0.0500	0.0600
	Sch.2	Avg	3.0733	3.0361	2.4320	2.2468	2.6287	3.0112	2.8591	3.1665
		RMSE	1.5074	1.4077	2.0734	2.0853	2.0827	1.1064	1.0845	1.1608
		RB	0.0244	0.0120	0.1893	0.2500	0.1200	0.0037	0.0500	0.0600
	Sch.3	Avg	3.1584	3.2552	2.5072	2.3500	2.6671	3.0299	2.8700	3.1955
		RMSE	1.5976	1.5722	2.1247	2.1190	2.1452	1.0900	1.0606	1.1519
		RB	0.0528	0.0851	0.1643	0.2200	0.1100	0.0100	0.0400	0.0700
	Sch.4	Avg	2.9309	2.8805	2.2926	2.1375	2.4544	2.9092	2.7593	3.0618
		RMSE	1.5531	1.4300	2.1900	2.1889	2.1992	1.0662	1.0634	1.0945
		RB	0.0230	0.0398	0.2358	0.2900	0.1800	0.0303	0.0800	0.0200
$(100, 70)$	Sch.1	Avg	3.0399	3.1030	2.2936	2.1307	2.4655	3.0083	2.8487	3.1692
		RMSE	1.4542	1.4628	2.0123	2.0296	2.0089	1.0493	1.0244	1.1052
		RB	0.0133	0.0343	0.2355	0.2900	0.1800	0.0028	0.0500	0.0600
	Sch.2	Avg	3.0791	3.0884	2.5252	2.3634	2.6957	3.0375	2.8905	3.1880
		RMSE	1.5008	1.3427	2.0200	2.0248	2.0284	1.2183	1.1874	1.2697
		RB	0.0264	0.0295	0.1583	0.2100	0.1000	0.0125	0.0400	0.0600
	Sch.3	Avg	3.1232	3.1737	2.4937	2.3233	2.6754	2.9741	2.8318	3.1208
		RMSE	1.3495	1.3469	1.9196	1.9285	1.9281	1.0471	1.0272	1.0917
		RB	0.0411	0.0579	0.1688	0.2300	0.1100	0.0086	0.0600	0.0400
	Sch.4	Avg	2.9834	2.9780	2.3157	2.1516	2.4875	2.9074	2.7616	3.0555
		RMSE	1.2857	1.2024	1.8625	1.8930	1.8452	0.9258	0.9217	0.9612
		RB	0.0055	0.0073	0.2281	0.2800	0.1700	0.0309	0.0800	0.0200
$(200, 100)$	Sch.1	Avg	2.9100	2.9386	2.1268	1.9754	2.2821	2.8911	2.7592	3.0249
		RMSE	1.2443	1.2555	1.9211	1.9512	1.8988	0.9155	0.9199	0.9310
		RB	0.0300	0.0205	0.2911	0.3400	0.2400	0.0363	0.0800	0.0100
	Sch.2	Avg	2.8227	2.8668	2.3326	2.1872	2.4829	2.9339	2.8118	3.0577
		RMSE	1.2312	1.0460	1.6599	1.6879	1.6458	0.8421	0.8377	0.8654
		RB	0.0591	0.0444	0.2225	0.2700	0.1700	0.0220	0.0600	0.0200
	Sch.3	Avg	3.0518	3.0979	2.4813	2.3155	2.6512	2.9538	2.8356	3.0757
		RMSE	1.1745	1.1385	1.6552	1.6873	1.6377	0.8944	0.8953	0.9121
		RB	0.0173	0.0326	0.1729	0.2300	0.1200	0.0154	0.0500	0.0300
	Sch.4	Avg	3.0054	2.9491	2.4945	2.3379	2.6565	2.9293	2.8131	3.0480
		RMSE	1.0441	0.9971	1.5006	1.5525	1.4655	0.8225	0.8234	0.8447
		RB	0.0018	0.0170	0.1685	0.2200	0.1100	0.0236	0.0600	0.0200

Table 6. *Cont.*

(n, r)	Sch.	Measures	Non-Bayesian		Bayesian					
			ML	MPS	Non-IP			IP		
					SE	LIN		SE	LIN	
						$\tau = 0.5$	$\tau = -0.5$		$\tau = 0.5$	$\tau = -0.5$
$(200, 140)$	Sch.1	Avg	3.0491	3.0710	2.5690	2.4049	2.7384	2.9325	2.8090	3.0578
		RMSE	1.0803	1.0890	1.5435	1.5884	1.5166	0.9277	0.9234	0.9503
		RB	0.0164	0.0237	0.1437	0.2000	0.0900	0.0225	0.0600	0.0200
	Sch.2	Avg	2.9620	2.9742	2.5609	2.4179	2.7083	2.9301	2.8176	3.0444
		RMSE	0.9560	0.8874	1.3854	1.4229	1.3661	0.7808	0.7798	0.8019
		RB	0.0127	0.0086	0.1464	0.1900	0.1000	0.0233	0.0600	0.0100
	Sch.3	Avg	2.9919	3.0252	2.5167	2.3757	2.6583	2.9099	2.7998	3.0213
		RMSE	1.0398	1.0098	1.4560	1.4891	1.4409	0.8384	0.8366	0.8584
		RB	0.0027	0.0084	0.1611	0.2100	0.1100	0.0300	0.0700	0.0100
	Sch.4	Avg	3.0546	3.0421	2.6801	2.5430	2.8199	2.9415	2.8323	3.0527
		RMSE	0.9185	0.8724	1.2904	1.3226	1.2744	0.7526	0.7579	0.7667
		RB	0.0182	0.0140	0.1066	0.1500	0.0600	0.0195	0.0600	0.0200

Table 7. Interval estimation at $\eta = 1.5$.

(n, r)	Sch.	Asy-CI				C-CI			
		ML		MPS		Non-IP		IP	
		AL	CP	AL	CP	AL	CP	AL	CP
$(100, 50)$	Sch.1	3.9669	91.30	5.0978	96.00	4.8511	95.30	4.1933	95.40
	Sch.2	3.9723	97.30	4.4908	98.30	3.8292	95.20	3.6945	95.20
	Sch.3	4.0224	95.00	4.6183	98.20	4.2337	95.40	3.7491	96.50
	Sch.4	4.0418	97.30	4.1896	98.20	3.9481	95.00	3.3572	95.00
$(100, 70)$	Sch.1	3.4406	92.30	4.4736	98.30	4.0581	95.30	3.4969	95.90
	Sch.2	4.0052	98.30	4.18	98.90	3.7449	95.00	3.6709	95.80
	Sch.3	3.5526	95.00	4.0874	97.60	3.6224	95.30	3.5855	95.20
	Sch.4	3.4021	94.00	3.9504	96.90	3.9395	95.20	3.3492	95.20
$(200, 100)$	Sch.1	3.2903	93.33	3.9173	97.33	3.7283	95.27	3.3874	95.32
	Sch.2	3.1681	95.33	3.4049	97.97	3.4248	95.24	3.3308	96.38
	Sch.3	3.0185	93.67	3.4255	96.93	3.2714	95.21	3.0017	95.07
	Sch.4	3.0123	95.67	3.1343	96.22	3.1363	95.17	2.9732	95.50
$(200, 140)$	Sch.1	2.8741	92.67	3.3921	97.67	3.1682	95.33	3.0918	95.69
	Sch.2	3.1814	96.00	3.2003	96.25	3.0873	95.22	2.9764	95.18
	Sch.3	2.8884	95.67	3.1556	97.00	2.9926	95.32	2.7684	95.06
	Sch.4	2.6618	92.67	2.9786	97.65	2.9186	95.29	2.8176	95.58

Table 8. Interval estimation at $\eta = 3.0$.

(n, r)	Sch.	Asy-CI				C-CI			
		ML		MPS		Non-IP		IP	
		AL	CP	AL	CP	AL	CP	AL	CP
$(100, 50)$	Sch.1	6.0590	97.00	6.1989	96.94	6.5888	95.24	3.9302	95.92
	Sch.2	5.1527	96.33	5.3652	97.67	5.8769	95.33	4.0306	96.33
	Sch.3	5.4113	96.67	5.5617	96.63	6.3835	95.29	3.8114	96.30
	Sch.4	4.6693	94.67	4.9554	96.67	6.1642	95.33	3.8919	96.30
$(100, 70)$	Sch.1	5.2310	98.33	5.3245	98.32	5.5444	95.30	3.8680	96.30
	Sch.2	4.7743	95.32	4.9354	95.65	5.8743	95.30	4.3126	95.32
	Sch.3	4.9676	97.00	5.0530	97.00	5.7158	95.33	3.7499	96.33
	Sch.4	4.6157	97.67	4.7183	97.65	5.1431	95.30	3.3610	96.64
$(200, 100)$	Sch.1	4.5177	96.70	4.5753	96.70	5.2294	95.30	3.1906	97.00
	Sch.2	3.7061	95.70	3.9551	97.70	4.6005	95.30	3.0899	96.00
	Sch.3	4.0586	95.30	4.1348	96.00	5.1036	95.30	3.2155	96.00
	Sch.4	3.6459	95.60	3.7428	96.70	4.6793	95.30	2.8018	95.70
$(200, 140)$	Sch.1	3.9742	96.70	3.9908	96.70	5.0981	95.70	3.1734	95.70
	Sch.2	3.6055	97.70	3.6837	98.30	4.4782	95.30	2.9590	96.30
	Sch.3	3.6442	98.00	3.6969	98.00	4.6904	95.30	2.9808	96.00
	Sch.4	3.4424	96.70	3.4879	97.70	4.5827	95.30	2.7998	98.30

8. Applications

In this section, two real-world datasets are used to demonstrate the efficiency of the TITL distribution in a data-fitting scenario. Thus, when we turn our view towards model tools, the TITL model is contrasted with many rival models, such as the TL model, PXL model (see [52]), IPL model (see [53]), Kw model (see [54]), B model (see [55]), TW model (see [56]), UW model (see [57]), EKw model (see [58]), UR model (see [59]), KMKw model (see [60]) and TKw model (see [61]).

We take into account nine well-referenced measures of goodness of fit to compare the related models, including the Kolmogorov–Smirnov statistic (KS), the Anderson–Darling statistics (A^*), the Hannan–Quinn information criterion (HQIC), the Akaike information criterion (AIC), the Bayesian information criterion (BIC), the consistent AIC (CAIC), and the Cramér–von Mises statistic (W^*). The model that meets these statistics and statistical measures in the lowest possible way is the one that is best. The p value (PKS) connected to the KS test is also extracted. A model with the highest PKS values is the best.

8.1. The First Dataset

To begin, we examine the number of months it takes for renal dialysis patients to become infected, as indicated by [62]. The times of infection data are: 12.5, 13.5, 3.5, 4.5, 5.5, 6.5, 6.5, 7.5, 3.5, 7.5, 12.5, 3.5, 2.5, 2.5, 7.5, 8.5, 9.5, 10.5, 11.5, 7.5, 14.5, 14.5, 21.5, 25.5, 27.5, 21.5, 22.5, and 22.5. We now execute a normalization operation by dividing these data by thirty, yielding values ranging from 0 to 1. The collected data are updated: 0.450000, 0.483333, 0.116667, 0.850000, 0.116667, 0.25000, 0.28333, 0.316667, 0.116667, 0.15000, 0.18333, 0.216667, 0.916667, 0.216667, 0.25000,0.25000, 0.08333, 0.08333,0.25000, 0.35000, 0.38333, 0.416667, 0.416667, 0.750000, 0.483333, 0.716667, 0.716667, and 0.750000.

Table 9 shows the MLEs with their standard errors (SErs) for this first dataset. Table 10 also displays the numerical values for the AIC, BIC, CAIC, HQIC, KS, PKS, W^*, and A^* statistics for the first dataset. Table 11 discusses the provided estimates, upper bounds (UBs), and lower bounds (LBs) of the CIs, in addition to the SErs for the TITL model's

parameters via PCT-II samples for the first dataset. Figure 8 shows the initial PDF shape mentioned using the non-parametric kernel density estimation approach. From Figure 8, we note that the shape of the PDF is asymmetric. Furthermore, the normality condition is checked via the quantile–quantile (QQ) plot in the same figure. The outliers can also be spotted using the box plot. Henceforth, we can say that there are outliers in the first dataset (the circle with red color in Figure 8 represents the median but the blue dots represents the data). Figure 9 demonstrates how the first dataset's profile log-likelihood behaves pretty clearly, as we can see that the root of the parameter is a global maximum. Figures 10 and 11 show the estimated PDFs and CDFs of the competitive models. Figure 12 displays the probability–probability (PP) plots of the competitive models for the first dataset. The charts in Figures 10–12 show that our model fits the data in a satisfying manner.

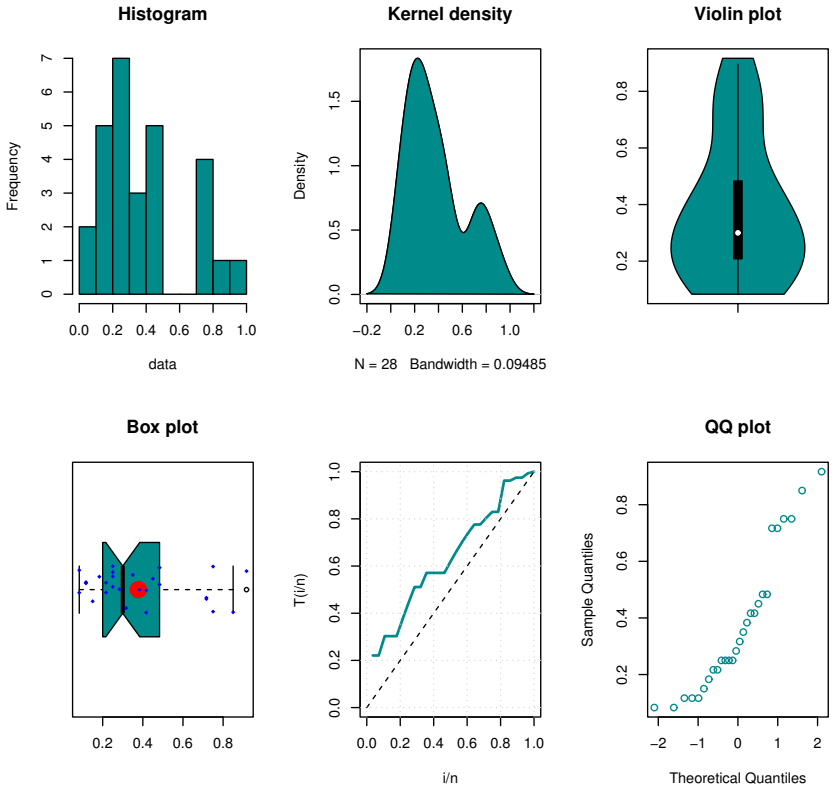

Figure 8. Some basic non-parametric plots for the first dataset.

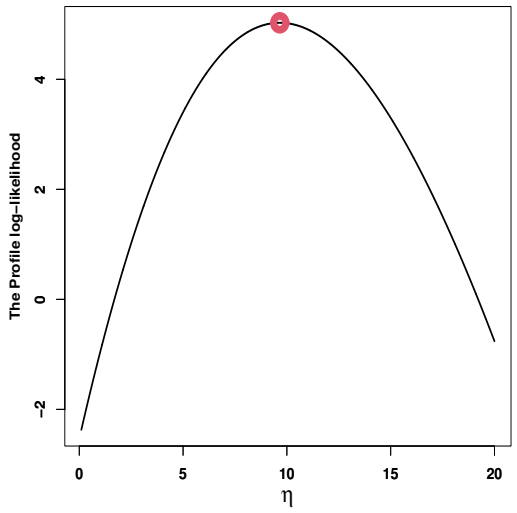

Figure 9. The profile log-likelihood of the TITL distribution for the first dataset.

Table 9. MLEs and SErs for the first dataset.

Distributions	MLE			SEr		
	η	β	α	η	β	α
TITL	9.6584	-	-	(2.7069)	-	-
TL	1.3778	-	-	(0.2604)	-	-
PXL	1.637	4.2239	-	(0.2409)	(0.9428)	-
IPL	1.1641	0.3153	-	(0.1421)	(0.0827)	-
Kw	1.265	2.0797	-	(0.2544)	(0.5714)	-
B	1.3567	2.1058	-	(0.3332)	(0.5496)	-
TW	3.3328	1.5218	-	(1.1901)	(0.2712)	-
UW	0.6124	1.6991	-	(0.1424)	(0.2669)	-
EKw	0.0146	1.7156	868.6461	(0.0135)	(0.2635)	(1354.074)
UR	0.5222	-	-	(0.0987)	-	-
KMKw	1.4419	1.867	-	(0.2706)	(0.5664)	-
TKw	1.3879	1.7814	0.4852	(0.2695)	(0.7043)	(0.4496)

Table 10. Measures of fitting for the first dataset.

Models	AIC	BIC	CAIC	HQIC	KS	PKS	W^*	A^*
TITL	−8.0555	−6.7233	−7.9017	−7.6482	0.11687	0.83901	0.0533	0.386
TL	−5.7049	−4.3727	−5.551	−5.2976	0.14415	0.60568	0.1067	0.6679
PXL	−3.5549	−0.8905	−3.0749	−2.7404	0.12081	0.80843	0.0627	0.465
IPL	0.2734	2.9378	0.7534	1.0879	0.13099	0.72263	0.1012	0.7071
Kw	−3.325	−0.6606	−2.845	−2.5104	0.13772	0.66296	0.1136	0.7049
B	−3.5552	−0.8908	−3.0752	−2.7407	0.14118	0.63213	0.1101	0.6859
TW	−4.8828	−2.2184	−4.4028	−4.0683	0.1195	0.81882	0.0712	0.4882
UW	−6.1223	−3.4579	−5.6423	−5.3077	0.124	0.78239	0.066	0.4415
EKw	−4.0392	−0.0426	−3.0392	−2.8174	0.12535	0.77113	0.067	0.4475
UR	−6.965	−5.6328	−6.8112	−6.5578	0.15798	0.48692	0.0857	0.4132
KMKw	−4.5907	−1.9263	−4.1107	−3.7762	0.12921	0.73815	0.09	0.5785
TKw	−2.2297	1.7669	−1.2297	−1.0079	0.12939	0.73658	0.0942	0.6043

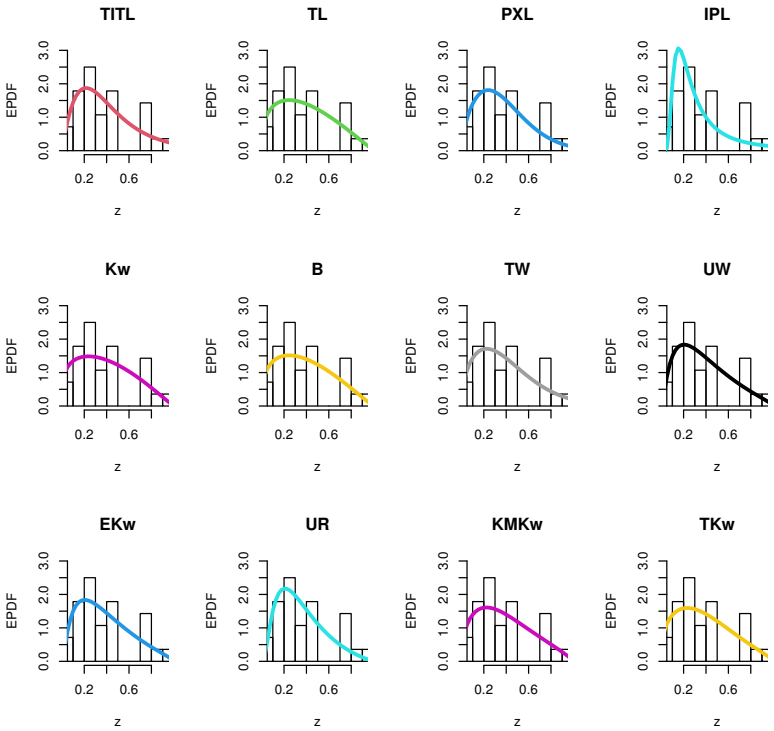

Figure 10. Estimated PDF plots of the competitive distributions for the first dataset.

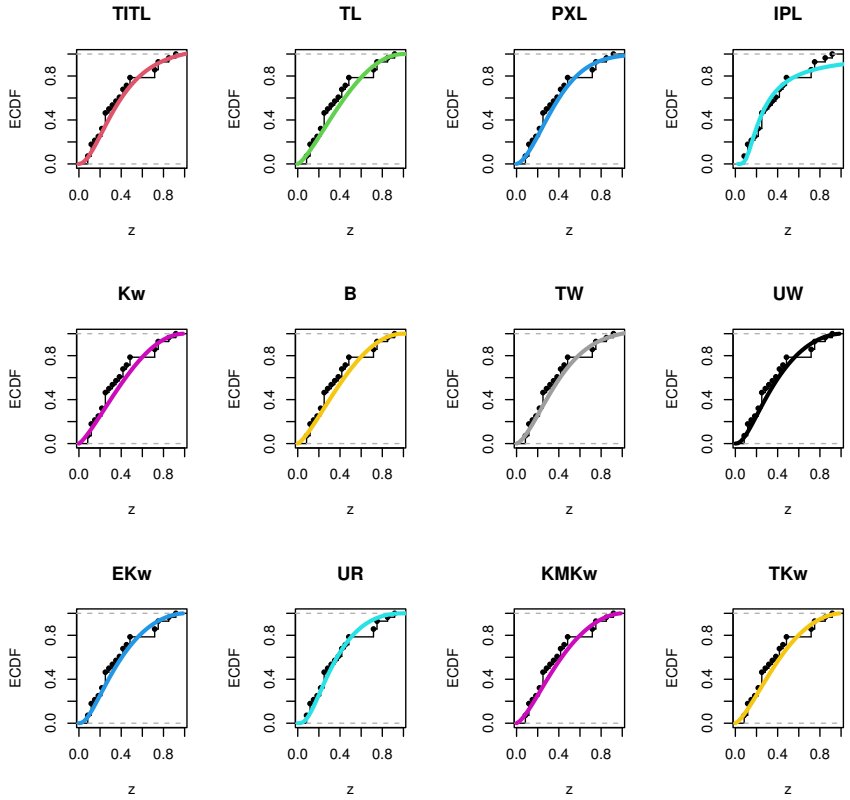

Figure 11. Estimated CDF plots of the competitive distributions for the first dataset.

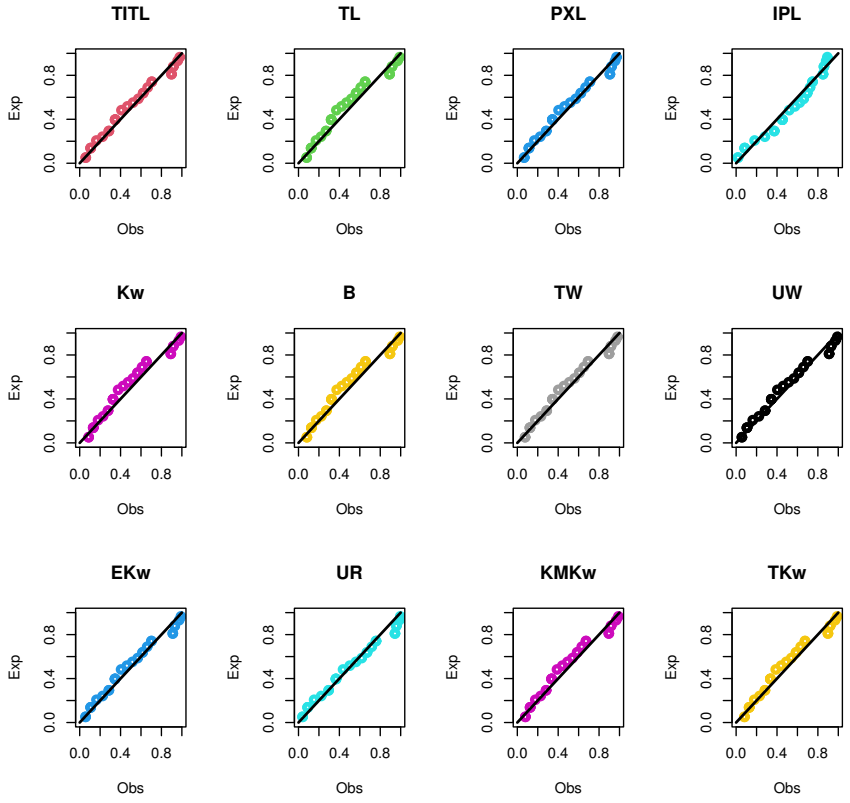

Figure 12. The PP plots of the fitted distributions for the first dataset.

Table 11. ML, MPS and BE for the TITL distribution under the PCT-II for the first dataset.

Sch.	Methods	Point Estimation		Interval Estimation	
		Estimate	SEr	LB	UB
Sch.1	ML	8.7305	2.8327	3.1784	14.2825
	MPS	8.4375	2.6270	3.2887	13.5863
	Bayesian at SE	6.7562	1.3419	4.1858	9.9519
	Bayesian at LIN $\tau = 0.5$	6.3493			
	Bayesian at LIN $\tau = -0.5$	7.2675			
Sch.2	ML	8.7305	2.8327	3.1784	14.2825
	MPS	8.4375	2.6270	3.2887	13.5863
	Bayesian at SE	6.7562	1.3419	4.1858	9.9519
	Bayesian at LIN $\tau = 0.5$	6.3493			
	Bayesian at LIN $\tau = -0.5$	7.2675			
Sch.3	ML	7.1133	2.6262	1.9661	12.2604
	MPS	6.7383	2.4336	1.9685	11.5081
	Bayesian at SE	4.9507	1.3278	2.4091	8.0893
	Bayesian at LIN $\tau = 0.5$	4.5502			
	Bayesian at LIN $\tau = -0.5$	5.4473			
Sch.4	ML	8.7305	2.8327	3.1784	14.2825
	MPS	8.4375	2.6270	3.2887	13.5863
	Bayesian at SE	6.7562	1.3419	4.1858	9.9519
	Bayesian at LIN $\tau = 0.5$	6.3493			
	Bayesian at LIN $\tau = -0.5$	7.2675			

8.2. The Second Dataset

The second dataset represents the trading economics credit rating of the 145 countries (2023). It shows the score of the creditworthiness of a country between 100 (riskless) and 0 (likely to default). We execute a normalization operation by dividing these data by 100, yielding values ranging from 0 to 1. The dataset was obtained from the following electronic address: https://tradingeconomics.com/country-list/rating (26 March 2023). The dataset is reported in Table 12.

Table 13 shows the MLEs with their SErs for this second dataset. Table 14 also displays the numerical values for the AIC, BIC, CAIC, HQIC, KS, PKS, W^*, and A^* statistics. Table 15 discusses the provided estimates, UBs and LBs of the CIs, in addition to the SErs for the TITL model's parameters via the PCT-II samples for the second dataset. Figure 13 shows the initial PDF shape mentioned using the non-parametric kernel density estimation approach for the second dataset. From Figure 13, we can note that the shape of the PDF is asymmetric. Furthermore, the normality condition is checked via the QQ plot in the same figure. The outliers can also be spotted using the box plot. Henceforth, we can say that there are outliers in the second dataset (the circle with red color in Figure 13 represents the median but the blue dots represents the data). Figure 14 demonstrates how the second dataset's profile log-likelihood behaves pretty clearly, as we can see that the root of the shape parameter is a global maximum. Figures 15 and 16 show the estimated PDFs and CDFs of the competitive models for the second dataset. Figure 17 shows the PP plots of the competitive models. The charts in Figures 15–17 show that our model fits the real data above well.

Table 12. The trading economics (TE) credit rating of 145 countries (2023).

Country	TE	Country	TE	Country	TE
Norway	99	Mauritius	60	Swaziland	30
Sweden	99	Mexico	60	Tanzania	30
European Union	98	Kazakhstan	58	Togo	30
Singapore	98	Panama	58	Zambia	30
United States	98	Uruguay	58	Cameroon	28
Austria	96	Cyprus	56	Mongolia	28
Finland	96	India	56	Turkey	28
New Zealand	95	Colombia	55	Bosnia and Herzegovina	27
France	92	Montserrat	55	Cape Verde	27
Hong Kong	90	Romania	55	Kyrgyzstan	27
Taiwan	90	Aruba	52	Papua New Guinea	27
United Arab Emirates	90	Azerbaijan	50	Angola	25
Belgium	87	Morocco	50	Bolivia	25
Isle of Man	87	San Marino	50	Gabon	25
Macau	87	Trinidad and Tobago	50	Madagascar	25
United Kingdom	87	Paraguay	48	Moldova	25
Qatar	86	Serbia	48	Nicaragua	25
South Korea	86	Greece	46	Solomon Islands	25
Cayman Islands	85	Georgia	45	St Vincent & Grenadines	25
Czech Republic	85	Guatemala	45	Tajikistan	25
Estonia	83	Macedonia	45	Iraq	23
Ireland	81	Vietnam	45	Nigeria	23
Israel	81	Oman	43	Tunisia	23
Kuwait	81	Brazil	42	Barbados	22
China	80	South Africa	41	Congo	22
Bermuda	78	Bangladesh	40	Maldives	22
Japan	77	Dominican Republic	40	Pakistan	21
Lithuania	76	Ivory Coast	40	Burkina Faso	20
Saudi Arabia	76	Namibia	40	Ecuador	20
Slovakia	76	Uzbekistan	38	Mozambique	18
Chile	75	Bahamas	37	Republic of the Congo	18
Iceland	75	Honduras	37	Belize	17
Malta	75	Senegal	37	El Salvador	16
Slovenia	75	Jordan	36	Ethiopia	16
Latvia	73	Albania	35	Ghana	16
Portugal	72	Fiji	35	Argentina	15
Poland	71	Montenegro	35	Cuba	15
Spain	71	Seychelles	35	Laos	15
Malaysia	68	Turkmenistan	35	Mali	15
Botswana	67	Bahrain	33	Suriname	15
Thailand	65	Benin	33	Ukraine	15
Andorra	63	Jamaica	33	Armenia	14
Italy	62	Rwanda	33	Russia	14
Bulgaria	61	Costa Rica	31	Belarus	11
Peru	61	Uganda	31	Lebanon	11
Philippines	61	Cambodia	30	Sri Lanka	11
Croatia	60	Egypt	30	Venezuela	11
Hungary	60	Kenya	30		
Indonesia	60	Lesotho	30		

https://tradingeconomics.com/country-list/rating (26 March 2023.)

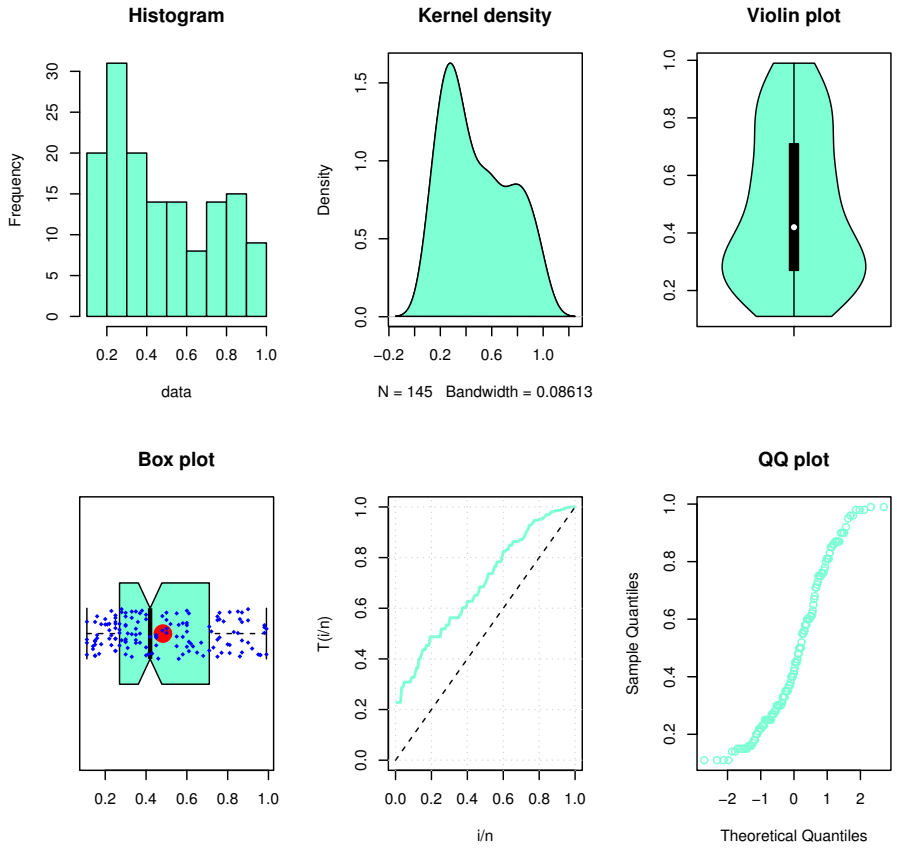

Figure 13. Some basic non-parametric plots for the second dataset.

Table 13. MLEs and SErs for the second dataset.

Distributions	MLE			SEr		
	η	β	α	η	β	α
TITL	4.0725	-	-	(1.0342)	-	-
TL	2.0397	-	-	(0.1694)	-	-
PXL	1.989	3.4907	-	(0.1317)	(0.3172)	-
IPL	1.3356	0.3777	-	(0.0714)	(0.0403)	-
Kw	1.3552	1.3722	-	(0.1319)	(0.1534)	-
B	1.4096	1.3895	-	(0.1555)	(0.153)	-
TW	2.0867	1.7079	-	(0.4652)	(0.1568)	-
UW	1.0519	1.3462	-	(0.0902)	(0.0939)	-
EKw	0.0084	1.3441	647.545	(0.0032)	(0.0925)	(401.9746)
UR	0.8683	-	-	(0.0721)	-	-
KMKw	1.5544	1.1978	-	(0.1402)	(0.1478)	-
TKw	1.4985	1.1078	0.5516	(0.1396)	(0.1999)	(0.2078)

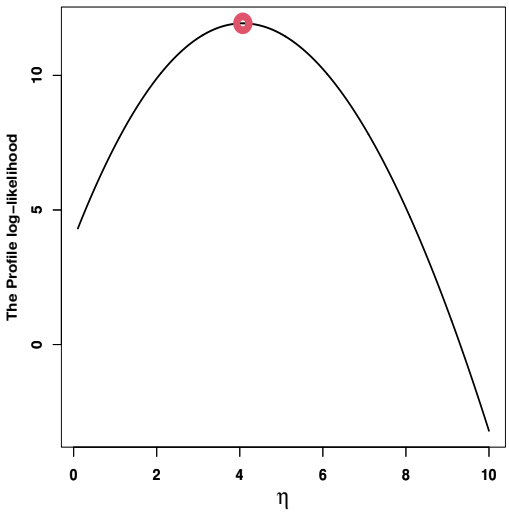

Figure 14. The profile log-likelihood of the TITL distribution for the second dataset.

Table 14. Measures of fitting for the second dataset.

Models	AIC	BIC	CAIC	HQIC	KS	PKS	W^*	A^*
TITL	−21.8691	−18.8924	−21.8411	−20.6596	0.0706	0.46518	0.2192	1.3184
TL	6.6854	9.6622	6.7134	7.895	0.11114	0.05564	0.3701	2.2434
PXL	1.7966	7.7501	1.8812	4.2157	0.09056	0.1853	0.2868	1.8143
IPL	36.2007	42.1542	36.2852	38.6198	0.12858	0.01655	0.4778	3.3536
Kw	−5.387	0.5664	−5.3025	−2.968	0.11684	0.03817	0.4012	2.4364
B	−5.9722	−0.0187	−5.8877	−3.5531	0.11783	0.03567	0.3947	2.3972
TW	−15.6395	−9.686	−15.555	−13.2204	0.09274	0.16499	0.2733	1.6344
UW	−13.9249	−7.9714	−13.8404	−11.5058	0.10304	0.09199	0.291	1.7599
EKw	−11.7021	−2.7719	−11.5319	−8.0735	0.10306	0.09188	0.2948	1.7832
UR	22.2578	25.2345	22.2857	23.4673	0.16523	0.00073	0.2738	1.7402
KMKw	−12.3769	−6.4234	−12.2924	−9.9578	0.10565	0.07854	0.3144	1.9033
TKw	−8.9	0.0302	−8.7298	−5.2713	0.10629	0.07554	0.336	2.0198

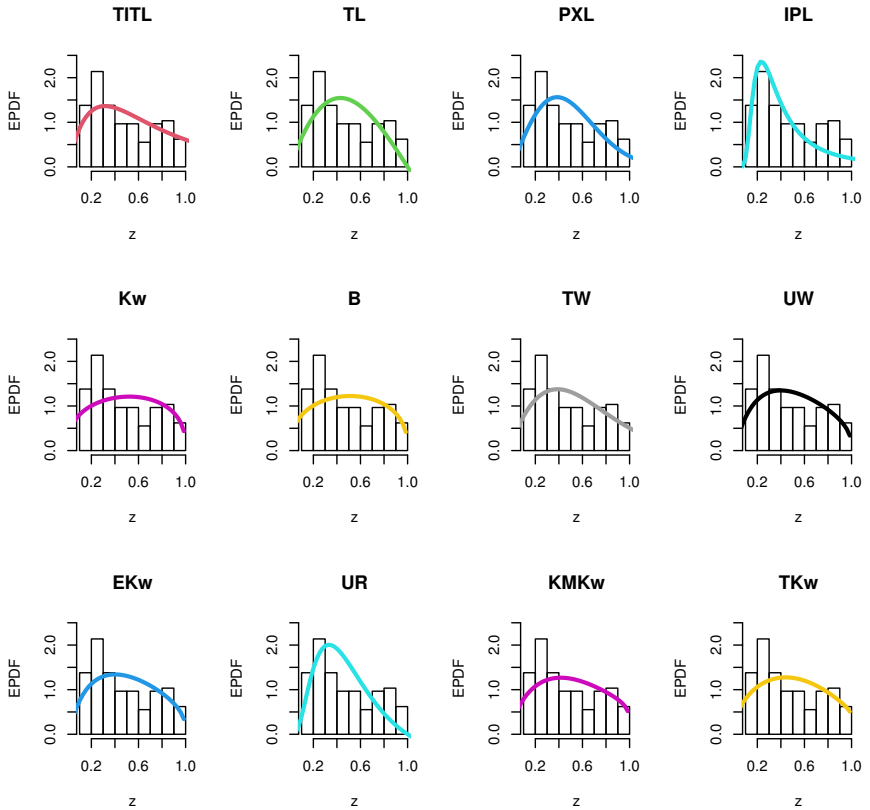

Figure 15. Estimated PDF plots of the competitive distributions for the second dataset.

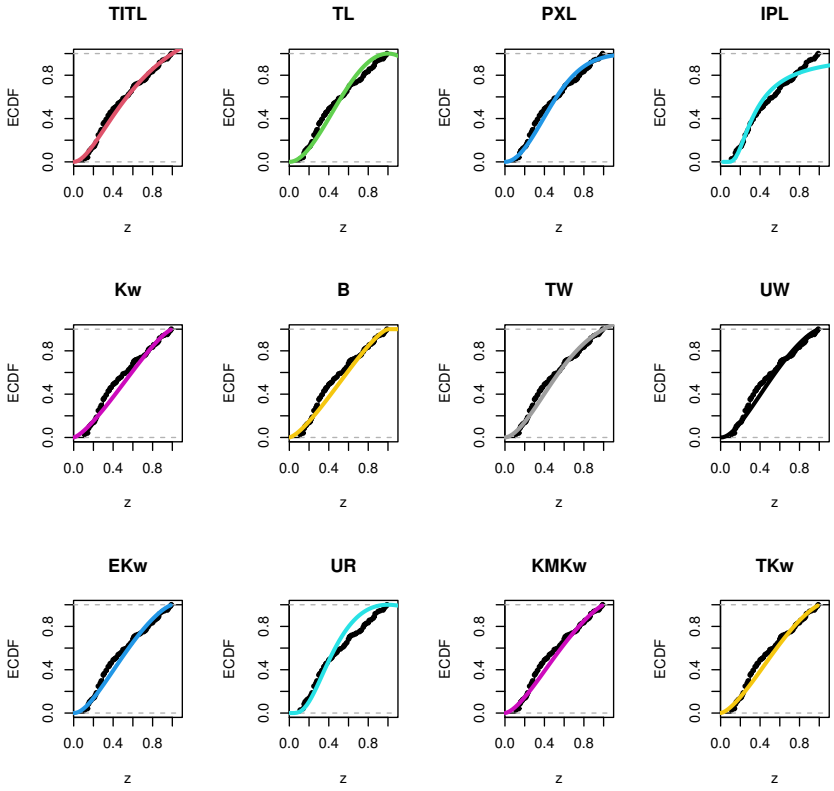

Figure 16. Estimated CDF plots of the competitive distributions for the second dataset.

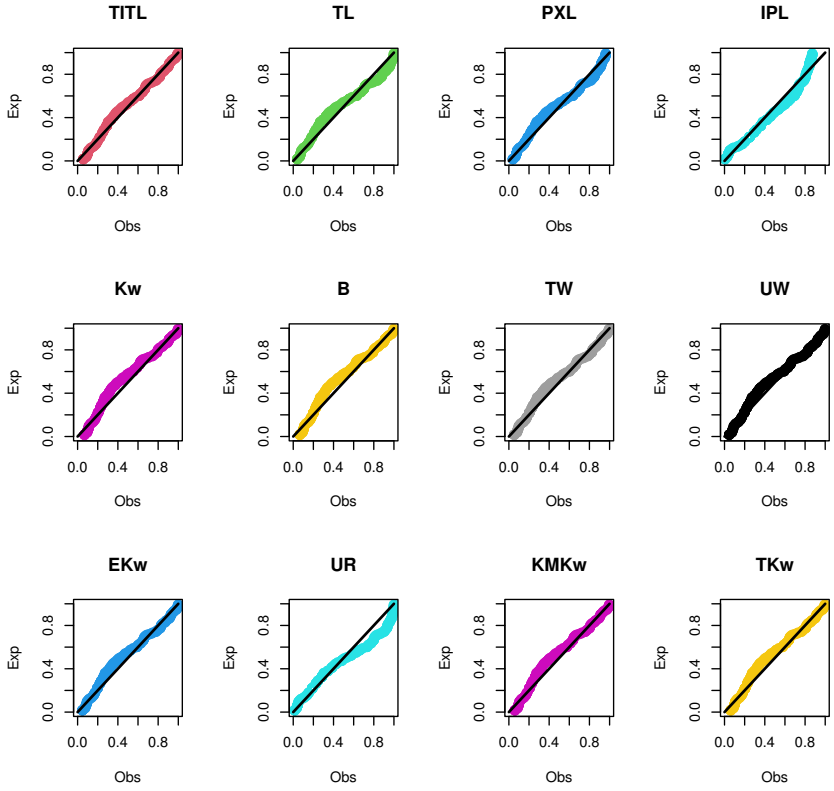

Figure 17. The PP plots of the fitted distributions for the second dataset.

Table 15. ML, MPS and BE for the TITL distribution under the PCT-II for the second dataset.

Sch.	Methods	Point Estimation		Interval Estimation	
		Estimate	SEr	LB	UB
Sch.1	ML	3.06563	1.5164	0.0936	6.0377
	MPS	3.12188	1.5297	0.1237	6.1200
	Bayesian at SE	0.50815	0.7391	0.0000	2.2492
	Bayesian at LIN $\tau = 0.5$	0.39678			
	Bayesian at LIN $\tau = -0.5$	0.67640			
Sch.2	ML	3.81×10^{-7}	0.1077	0.0000	0.2111
	MPS	1.34×10^{-6}	0.2080	0.0000	0.4076
	Bayesian at SE	0.00628	0.0291		0.0332
	Bayesian at LIN $\tau = 0.5$	0.00608			
	Bayesian at LIN $\tau = -0.5$	0.00650			
Sch.3	ML	0.00031	0.4417	0.0000	0.8661
	MPS	0.00031	0.9955	0.0000	1.9514
	Bayesian at SE	0.09273	0.2754	0.0000	0.8017
	Bayesian at LIN $\tau = 0.5$	0.07649			
	Bayesian at LIN $\tau = -0.5$	0.11514			
Sch.4	ML	3.81×10^{-7}	0.0239	0.0000	0.0467
	MPS	1.34×10^{-6}	0.2063	0.0000	0.4043
	Bayesian at SE	0.00524	0.0184	0.0000	0.0298
	Bayesian at LIN $\tau = 0.5$	0.00516			
	Bayesian at LIN $\tau = -0.5$	0.00533			

9. Conclusions

In this article, we investigated and studied a new asymmetric distribution with one shape parameter in the domain $[0, 1]$, called the truncated inverse Topp–Leone distribution. As evidence of its functional interest, its probability density function can be unimodal or right-skewed. On the other hand, the hazard rate function can be increased. Some important statistical properties, such as the mode, quantile function, median, Bowley's skewness, Moor's kurtosis, moments, incomplete moments, Lorenz and Bonferroni curves, probability-weighted moments, and numerical tables, were determined. Several different measures of uncertainty, such as the Rényi entropy, Tsallis entropy, Arimoto entropy, Havrda and Charvat entropy, Awad and Alawneh 1 entropy, Awad and Alawneh 2 entropy, Mathai–Haubold entropy, extropy, and residual extropy, were computed. To estimate the model parameters under progressive type-II censoring, the maximum likelihood, maximum product spacing, Bayesian using the squared error and Linex loss functions, were employed. Two applications employing real-world datasets explained the significance of the new truncated model in comparison to existing statistical models such as the Topp–Leone, power XLindley, inverse power Lindley, Kumaraswamy, beta, truncated Weibull, unit-Weibull, exponentiated Kumaraswamy, unit-Rayleigh, Kavya–Manoharan Kumaraswamy, and transmuted Kumaraswamy models. Finally, it is important to point out that one of the limitations of the progressive type-II censoring is that the time of the experiment can be very long if the units are highly reliable. As a result, more advanced schemes will need to be utilized in future studies.

Author Contributions: Conceptualization, M.E., N.A., A.S.H., C.C. and A.H.A.-H.; methodology, M.E., N.A., A.S.H., C.C. and A.H.A.-H.; software, M.E., N.A., A.S.H., C.C. and A.H.A.-H.; validation, M.E., N.A., A.S.H., C.C. and A.H.A.-H.; formal analysis, M.E., N.A., A.S.H., C.C. and A.H.A.-H.; investigation, M.E., N.A., A.S.H., C.C. and A.H.A.-H.; resources, M.E., N.A., A.S.H., C.C. and A.H.A.-H.; data curation, M.E., N.A., A.S.H., C.C. and A.H.A.-H.; writing-original draft preparation, M.E., N.A., A.S.H., C.C. and A.H.A.-H.; writing-review and editing, M.E., N.A., A.S.H., C.C. and A.H.A.-H.; visualization, M.E., N.A., A.S.H., C.C. and A.H.A.-H. All authors have read and agreed to the published version of the manuscript.

Funding: This research was funded by King Saud University, grant number RSPD2023R548.

Data Availability Statement: Not applicable.

Acknowledgments: Researchers Supporting Project number (RSPD2023R548), King Saud University, Riyadh, Saudi Arabia.

Conflicts of Interest: The authors declare no conflict of interest.

References

1. Topp, C.W.; Leone, F.C. A family of J-shaped frequency functions. *J. Am. Stat. Assoc.* **1955**, *50*, 209–219. [CrossRef]
2. Al-Shomrani, A.; Arif, O.; Shawky, A.; Hanif, S.; Shahbaz, M.Q. Topp-Leone family of distributions: Some properties and application. *Pak. J. Stat. Oper. Res.* **2016**, *12*, 443–451. [CrossRef]
3. Rezaei, S.; Sadr, B.B.; Alizadeh, M.; Nadarajah, S. Topp-Leone generated family of distributions: Properties and applications. *Commun. Stat. Theory Methods* **2016**, *46*, 2893–2909. [CrossRef]
4. Sangsanit, Y.; Bodhisuwan, W. The Topp-Leone generator of distributions: Properties and inferences. *Songklanakarin Sci. Technol.* **2016**, *38*, 537–548.
5. Yousof, H.M.; Alizadeh, M.; Jahanshahi, S.M.A.; Ramires, T.G.; Ghosh, I.; Hamedani, G.G. The Transmuted Topp-Leone G family of distributions: Theory, characterizations and applications. *J. Data Sci.* **2017**, *15*, 723-740. [CrossRef]
6. Reyad, H.; Korkmaz, M.C.; Afify, A.Z.; Hamedani, G.G.; Othman, S. The Fréchet Topp-Leone-G family of distributions: Properties, characterizations and applications. *Ann. Data Sci.* **2019**, *8*, 345–366. [CrossRef]
7. Reyad, H.M.; Alizadeh, M.; Jamal, F.; Othman, S.; Hamedani, G.G. The exponentiated generalized Topp Leone-G family of distributions: Properties and applications. *Pak. J. Stats. Oper. Res.* **2019**, *15*, 1–24. [CrossRef]
8. Mahdavi, A. Generalized Topp-Leone family of distributions. *Biostat. Epidemiol.* **2017**, *3*, 65–75.
9. Elgarhy, M.; Nasir, M.A.; Jamal, F.; Ozel, G. The type II Topp-Leone generated family of distributions: properties and applications. *J. Stat. Manag. Syst.* **2018**, *21*, 1529–1551. [CrossRef]
10. Bantan, R.A.; Jamal, F.; Chesneau, C.; Elgarhy, M. A new power Topp-Leone generated family of distributions with applications. *Entropy* **2019**, *21*, 1177. [CrossRef]
11. Elgarhy, M.; Hassan, A.S.; Nagy, H. Parameter estimation methods and applications of the power Topp-Leone distribution. *Gazi Univ. J. Sci.* **2022**, *35*, 731–746. [CrossRef]
12. Alizadeh, M.; Lak, F.; Rasekhi, M.; Ramires, T.G.; Yousof, H.M.; Altun, E. The odd log-logistic Topp-Leone G family of distributions: Heteroscedastic regression models and applications. *Comput. Stat.* **2018**, *33*, 1217–1244. [CrossRef]
13. Chipepa, F.; Oluyede, B.; Peter, O.P. The Burr III-Topp-Leone-G family of distributions with applications. *Heliyon* **2021**, *7*, e06534. [CrossRef]
14. Hassan, A.S.; Elgarhy, M.; Ragab, R. Statistical properties and estimation of inverted Topp-Leone distribution. *J. Stat. Appl. Probab.* **2020**, *9*, 319–331.
15. Metwally, A.S.M.; Hassan, A.S.; Almetwally, E.M.; Kibria, B.M.G.; Almongy, H.M. Reliability analysis of the new exponential inverted Topp-Leone distribution with applications. *Entropy* **2021**, *23*, 1662. [CrossRef]
16. Almetwally, E.M.; Alharbi, R.; Alnagar, D.; Hafez, E.H. A new inverted Topp-Leone distribution: Applications to the COVID-19 mortality rate in two different countries. *Axioms* **2021**, *10*, 25. [CrossRef]
17. Mohamed, R.A.H.; Elgarhy, M.; Alabdulhadi, M.H.; Almetwally, E.M.; Radwan, T. Statistical inference of truncated Cauchy power-inverted Topp-Leone distribution under hybrid censored scheme with applications. *Axioms* **2023**, *12*, 148. [CrossRef]
18. Mahdavi, A.; Silva, O.G. A method to expand family of continuous distributions based on truncated distributions. *J. Stat. Res. Iran* **2017**, *13*, 231–247. [CrossRef]
19. Abid, S.H.; Abdulrazak, R.K. [0, 1] truncated Fréchet-G generator of distributions. *Appl. Math.* **2017**, *7*, 51–66.
20. Bantan, R.A.R.; Jamal, F.; Chesneau, C.; Elgarhy, M. Truncated inverted Kumaraswamy generated family of distributions with applications. *Entropy* **2019**, *21*, 1089. [CrossRef]
21. ZeinEldin, R.A.; Chesneau, C.; Jamal, F.; Elgarhy, M.; Almarashi, A.M.; Al-Marzouki, S. Generalized truncated Fréchet generated family distributions and their applications. *Comput. Model. Eng. Sci.* **2021**, *126*, 791–819.

22. Almarashi, A.M.; Jamal, F.; Chesneau, C.; Elgarhy, M. A new truncated Muth generated family of distributions with applications. *Complexity* **2021**, *2021*, 1211526. [CrossRef]
23. Balakrishnan, N.; Aggrawala, R. *Progressive Censoring, Theory, Methods and Applications*; Birkhauser: Boston, MA, USA, 2000.
24. Abdel-Hamid, A.H. Properties, estimations and predictions for a Poisson-half-logistic distribution based on progressively type-II censored samples. *Appl. Math. Model.* **2016**, *40*, 7164–7181. [CrossRef]
25. Kundu, D.; Joarder, A. Analysis of type-II progressively hybrid censored data. *Comput. Stat. Data Anal.* **2006**, *50*, 2509-2528. [CrossRef]
26. Mohammed, H.S.; Nassar, M.; Alotaibi, R.; Elshahhat, A. Analysis of adaptive progressive Type-II hybrid censored Dagum data with applications. *Symmetry* **2022**, *14*, 2146. [CrossRef]
27. Maiti, K.; Kayal, S. Estimation of parameters and reliability characteristics for a generalized Rayleigh distribution under progressive Type-II censored sample. *Commun. Stat-Simul. Comput.* **2021**, *50*, 3669-3698. [CrossRef]
28. Lee, K.; Cho, Y. Bayesian and maximum likelihood estimations of the inverted exponentiated half logistic distribution under progressive Type II censoring. *J. Appl. Stat.* **2017**, *44*, 811-832. [CrossRef]
29. Buzaridah, M.M.; Ramadan, D.A.; El-Desouky, B.S. Estimation of some lifetime parameters of flexible reduced logarithmic-inverse Lomax distribution under progressive Type-II censored data. *J. Math.* **2022**, *2022*, 1690458. [CrossRef]
30. Alotaibi, R.; Almetwally, E.M.; Kumar, D.; Rezk, H. Optimal test plan of step-stress model of alpha power Weibull lifetimes under progressively Type-II censored samples. *Symmetry* **2022**, *14*, 1801. [CrossRef]
31. Alotaibi, R.; Baharith, L.A.; Almetwally, E.M.; Khalifa, M.; Ghosh, I.; Rezk, H. Statistical inference on a Finite mixture of exponentiated Kumaraswamy-G distributions with progressive Type II censoring Using bladder cancer data. *Mathematics* **2022**, *10*, 2800. [CrossRef]
32. Wang, L.; Wu, K.; Zuo, X. Inference and prediction of progressive Type-II censored data from unit-generalized Rayleigh distribution. *Hacet. J. Math. Stat.* **2022**, *51*, 1752-1767. [CrossRef]
33. Tse, S.K.; Yang, C.; Yuen, H.K. Statistical analysis of Weibull distributed lifetime data under type II progressive censoring with binomial removals. *J. Appl. Stat.* **2020**, *27*, 1033-1043. [CrossRef]
34. Salem, S.; Abo-Kasem, O. E.; Hussien, A. On joint Type-II generalized progressive hybrid censoring scheme. *Comput. J. Math. Stat. Sci.* **2023**, *2*, 123-158. [CrossRef]
35. Kleiber, C.; Kotz, S. *Statistical Size Distributions in Economics and Actuarial Sciences*; Wiley: New York, NY, USA, 2023.
36. Greenwood, J.A.L.; wehr, J.M.; Wallis, J.R.; Matals, N.C. Probability weighted moments: Definition and relation to parameters of several distributions expressable in inverse form. *Water Resour. Res.* **1979**, *15*, 1049–1054. [CrossRef]
37. Rényi A. On measures of entropy and information. In Proceedings of the 4th Berkeley Symposium on Mathematical Statistics and Probability, Berkeley, CA, USA, 20 June–30 July 1960; Volume 1, pp. 47–561.
38. Tsallis C. Possible generalization of Boltzmann-Gibbs statistics. *J. Stat. Phys.* **1988**, *52*, 479–487. [CrossRef]
39. Arimoto S. Information-theoretical considerations on estimation problems. *Inf. Control* **1971**, *19*, 181–194. [CrossRef]
40. Havrda, J.; Charvat, F. Quantification method of classification processes, concept of structural a-entropy. *Kybernetika* **1967**, *3*, 30–35.
41. Awad, A.M.; Alawneh, A.J. Application of entropy to a life-time model. *Ima J. Math. Control Inf.* **1987**, *4*, 143–148. [CrossRef]
42. Mathai, A.M.; Haubold, H.J. On generalized distributions and pathways. *Phys. Lett.* **2008**, *372*, 2109–2113. [CrossRef]
43. Lad, F.; Sanfilippo, G.; Agro, G. Extropy: Complementary dual of entropy. *Stat. Sci.* **2015**, *30*, 40–58. [CrossRef]
44. Shannon, C.E. A mathematical theory of communication. *Bell Syst. Tech. J.* **1948**, *27*, 379–423. [CrossRef]
45. Qiu, G.; Jia, K. The residual extropy of order statistics. *Stat. Probab. Lett.* **2018**, *133*, 15–22. [CrossRef]
46. Cohen, A.C. Progressively censored samples in life testing. *Technometrics* **1963**, *5*, 327–329. [CrossRef]
47. Cheng, R.C.H.; Amin, N.A.K. Estimating parameters in continuous univariate distributions with a shifted origin. *J. R. Stat. Soc. Ser. B.* **1983**, *45*, 394–403. [CrossRef]
48. Coolen, F.P.A.; Newby, M.J. *A Note on the Use of the Product of Spacings in Bayesian Inference*; Department of Mathematics and Computing Science University of Technology: Eindhoven, The Netherlands, 1990.
49. Anatolyev, S.; Kosenok, G. An alternative to maximum likelihood based on spacings. *Econ. Theory* **2005**, *21*, 472–476. [CrossRef]
50. Ng, H.K.T.; Luo, L.; Hu, Y.; Duan, F. Parameter estimation of three-parameter Weibull distribution based on progressively type-II censored samples. *Stat Comput. Simul.* **2012**, *82*, 1661–1678. [CrossRef]
51. Dey, S.; Dey, T.; Luckett, D.J. Statistical inference for the generalized inverted exponential distribution based on upper record values. *Math. Comput. Simul.* **2016**, *120*, 64–78. [CrossRef]
52. Meriem, B.; Gemeay, A.M.; Almetwally, E.M.; Halim, Z.; Alshawarbeh, E.; Abdulrahman, A.T.; Hussam, E. The power xlindley distribution: Statistical inference, fuzzy reliability, and covid-19 application. *J. Funct. Spaces* **2022**, *2022*, 9094078. [CrossRef]
53. Barco, K.V.P.; Mazucheli, J.; Janeiro, V. The inverse power Lindley distribution. *Commun. Stat.-Simul. Comput.* **2017**, *46*, 6308–6323. [CrossRef]
54. Kumaraswamy, P. A Generalized Probability Density Function for Double-Bounded Random Processes. *J. Hydrol.* **1980**, *46*, 79–88. [CrossRef]
55. Gupta, A.K.; Nadarajah, S. *Handbook of Beta Distribution and Its Applications*; CRC Press: Boca Raton, FL, USA, 2004.
56. Najarzadegan, H.; Alamatsaz, M.H.; Hayati, S. Truncated Weibull-G more flexible and more reliable than beta-G distribution. *Int. J. Stat. Probab.* **2017**, *6*, 1–17. [CrossRef]
57. Mazucheli, J.; Menezes, A.F.B.; Ghitany, M.E. The unit-Weibull distribution and associated inference. *J. Appl. Probab. Stat.* **2018**, *13*, 1–22.

58. Lemonte, A.J.; Barreto-Souza, W.; Cordeiro, G.M. The exponentiated Kumaraswamy distribution and its log-transform. *Braz. J. Probab. Stat.* **2013**, *27*, 3153. [CrossRef]
59. Bantan, R.A.; Chesneau, C.; Jamal, F.; Elgarhy, M.; Tahir, M.H.; Ali, A.; Anam, S. Some new facts about the unit-Rayleigh distribution with applications. *Mathematics* **2020**, *8*, 1954. [CrossRef]
60. Alotaibi, N.; Elbatal, I.; Shrahili, M.; Al-Moisheer, A.S.; Elgarhy, M.; Almetwally, E.M. Statistical inference for the Kavya-Manoharan Kumaraswamy model under ranked set sampling with applications. *Symmetry* **2023**, *15*, 587. [CrossRef]
61. Khan, M.S.; King, R.; Hudson, I.L. Transmuted Kumaraswamy distribution. *Stat. Transit. New Ser.* **2016**, *2*, 183–210. [CrossRef]
62. Klein, J.P.; Moeschberger, M.L. *Survival Analysis: Techniques for Censored and Truncated Data*; Springer: Berlin/Heidelberg, Germany, 2006.